Toxicological Assessment of Particulate Emissions from the Exhaust of Old and New Model Heavy- and Light-Duty Vehicles

Katharine Moore, PhD
Andrea Polidori, PhD
Constantinos Sioutas, ScD

Sonny Astani Department of Civil and Environmental Engineering
University of Southern California
3620 South Vermont Avenue
Los Angeles, CA 90089

METRANS
Transportation Center
USC | CSULB

Disclaimer

The contents of this report reflect the views of the authors, who are responsible for the facts and the accuracy of the information presented herein. The document is disseminated under the sponsorship of the Department of Transportation, University Transportation Centers Program, and California Department of Transportation in the interest of information exchange. The U.S. Government and California Department of Transportation assume no liability for the contents or use thereof. The contents do not necessarily reflect the official views or policies of the State of California or the Department of Transportation. This report does not constitute a standard, specification, or regulation.

Abstract

The primary objective of this project is to develop an improved understanding of the factors affecting the toxicology of particulate exhaust emissions. Diesel particulate matter is a known carcinogen, and particulate exhaust emissions from both light-duty and heavy-duty vehicles are toxic. Particulate matter emissions from three light-duty vehicles in five different configurations [a Honda Accord operating with diesel with a closed-coupled oxidation catalyst and an underfloor catalyst replaced in some tests with a diesel particle filter (DPF), a Toyota Corolla operating with gasoline, and a VW Golf alternatively operating with petrodiesel or biodiesel] were tested in a dynamometer facility. The vehicles were tested using a variety of real-world driving cycles and emission controls range from none through compliance with the 2007 and 2010 EPA standards. The chemical composition of the PM was fully characterized and the oxidative potential of the emissions assessed using two different toxicity assays. The DPF-equipped Accord and the gasoline vehicle had the lowest overall PM emission rates and the diesel and biodiesel vehicles produced the most potent exhaust in terms of oxidative activity. Correlations were explored between the chemical composition of the PM and the assay results. While there may be some confounding effects, elevated organic species emissions and select metals (associated with lube oil) were found to be correlated with the oxidative potential of the PM. These data, in combination with knowledge of the physical exhaust emission properties, emission control level and driving cycle provide insight into the expected toxicological impacts of changes in the vehicle fleet and planned emission control strategies and will be useful in the evaluation of the effect of fleet turn-over on the air quality impacts in the Los Angeles basin.

Keywords: Diesel emissions, gasoline emissions, oxidative stress, particulate matter health effects

Introduction

Air quality in the Los Angeles area is routinely among the worst – if not the worst – in the United States due to high atmospheric ozone and particulate matter concentrations. The principal source of particulate matter (PM) emissions in Los Angeles is from combustion, principally from motor vehicles (Kim et al., 2002, Westerdahl et al., 2005). Vehicle miles traveled by all classes of motor vehicles in the Los Angeles air basin (LAB) are expected to continue to increase in the future. Therefore, motor vehicles in the LAB will continue to be the primary source of directly-emitted PM and also the reactive gas-phase precursor species that through atmospheric processing produces secondary PM. Other pollutant sources – such as food cooking and wood burning – also contribute to a lesser degree to the high atmospheric PM concentrations in Los Angeles (Kleeman et al., 1999, Schauer et al., 2001).

Elevated levels of PM concentrations, particularly fine PM or $PM_{2.5}$ (less than 2.5 micrometers in diameter), are associated with adverse human health impacts (Dockery and Pope, 2006). Determining the relationship between particle size and composition and specific health endpoints is, however, an active area of research. Motor vehicle-related pollution is implicated in some adverse health outcomes. For example, children living within 500 m of a freeway in Los Angeles are more likely to have reduced lung function compared to those who lived at least 1500 m away (Gauderman et al., 2007). Further, the state of California classified diesel PM as a toxic contaminant in 1998 due to its carcinogenicity and association with specific respiratory and cardiovascular health problems (Stayner et al., 1998, Mills et al., 2005, Kleinman et al., 2005). Recent work suggests that pro-inflammatory response at the cellular level as well as increased incidence of asthma, among other diseases, are linked to exposure to ultrafine particles (approximately < 0.10 micrometers in diameter) such as those emitted by motor vehicle combustion (Pekkanen et al., 1997, Li et al., 2003, Xia et al., 2004, Delfino et al., 2005). Substantial evidence suggests that it is the ability of ultrafine or quasi-ultrafine particles to induce oxidative stress in cells through the production of reactive oxygen species (ROS) that leads to the adverse health outcomes observed (Li et al., 2003, Nel, 2005). High levels of ROS change the redox status of the cell (Schafer et al., 2003), thereby triggering a cascade of events associated with inflammation and, at higher concentrations, apoptosis (cell death) (Li et al., 2002, 2003). Both chemical and biological toxicological

assays – described in detail below – are available to quantitatively characterize the production of ROS (Cho et al., 2005, Landreman et al., 2008).

The Southern California Particle Center – a US EPA-funded research center located at the University of Southern California – and the USC Aerosol Laboratory have been leaders in investigating the impact of motor vehicles on air quality and PM concentrations in the LAB including health effects. One goal is to link the chemical characteristics and physical properties of motor vehicle PM to adverse health outcomes in order to design more effective emission control technologies for motor vehicles. A major objective of an on-going California Air Resources Board (ARB)-funded study being conducted by the USC Aerosol Lab is to determine the physicochemical and toxicological properties of the semi-volatile and non-volatile fractions of PM from heavy-duty diesel and alternative fueled vehicles operated both with and without emission control technologies. Toxicity testing of vehicular emissions is not widespread. Further it is not well established how the toxicity (as quantified by the assays described below) changes as the chemical composition of the PM emissions varies between motor vehicles. In addition to heavy-duty diesel vehicles, light-duty diesel vehicles are in widespread use in Europe and are being re-introduced to the United States with the 2009 model year. The USC Aerosol Lab, in collaboration with the Laboratory of Applied Thermodynamics (LAT) at Aristotle University in Thessaloniki, Greece, was able to obtain PM samples from the emissions testing of several light-duty diesel passenger vehicles using different fuels and with varying emissions control technologies. Due to differences in operating characteristics, emissions from light-duty diesel vehicles are likely to be different from heavy-duty diesel vehicles (Ntziachristos et al, 2006). Therefore, it is necessary to evaluate the emissions from both heavy-duty and light-duty diesel vehicles.

Additionally, proposed European Union (EU) standards for PM emissions from motor vehicles are based entirely on number-based concentrations of the non-volatile PM fraction emitted. The semi-volatile PM fraction, however, may be very important in terms of its contribution to human exposure. Current emissions control technologies are effective at removing the non-volatile PM fraction, but less effective at controlling the volatile and semi-volatile fractions. In fact, removal of the non-volatile PM fraction can

increase the concentration of the volatile/semi-volatile aerosol fraction by promoting both new particle formation and existing particle growth by condensing organic vapors (Bagley et al., 1998, Kittelson, 1998). Understanding how the toxicity of vehicular PM varies with component particle volatility should direct the design of emissions control technologies in order to better protect public health. This information will be crucial in assessing the effectiveness of new emissions standards currently under consideration by the EU. Further, unequivocal demonstration of an increased toxicity in the volatile/semi-volatile nucleation PM mode from heavy- and light-duty engines, will raise significant concerns regarding the validity, effectiveness and overall wisdom of this standard, which may affect future regulations here in California.

The chemical composition and toxicological properties of PM emissions from the light-duty diesel passenger vehicles were fully analyzed and assessed through the generous funding of the METRANS Center (METRANS 2008 – 2009 grant "Toxicological assessment of particulate emissions from the exhaust of old and new model heavy- and light-duty vehicles"). The results are reported below and include relevant non-regulated pollutants. These results are either published or pending publication in the peer-reviewed technical press (see the "Project Publications" section below). This new work should aid the development of the most effective policies to control/mitigate particulate matter emissions from light-duty passenger diesel vehicles. Diesel fuel use by passenger vehicles is projected to grow substantially in the future. The outcome of this study will be very helpful in assessing the health consequences of population exposure to traffic sources in Los Angeles, where on average some 9 million individuals spend 2-3 hours per day commuting in heavily congested freeways.

Study Methodology

Experiments to collect "typical" PM emissions from light-duty diesel passenger vehicles spanning the range of European emissions standards were conducted at the light-duty dynamometer facility of the Laboratory of Applied Thermodynamics at Aristotle Univeristy in Thessaloniki, Greece. Funding for the

dynamometer testing was obtained separately by our colleagues from the Greek Secretariat for Research and Technology (Contract No. 05NON-EU-137).

Three vehicles in a total of five configurations were tested (see Table 1). The newest vehicle was a 2.2 L "Euro 4" compliant diesel passenger car (the Honda Accord 2.2i-CTDi) equipped with exhaust gas recirculation and a three-stage oxidation aftertreatment system. This consisted of a closed-coupled oxidation catalyst (precatalyst) and a main underfloor catalyst formed of two monoliths in series. The same vehicle was also tested in an alternative configuration, with its main oxidation catalyst replaced by a diesel particle filter (DPF). The DPF was a Pt-coated SiC filter of octagonal channel cross-section with 300 cells/in^2. In this configuration, the vehicle complied with the "Euro 5" (2010) PM emission standards. It is therefore designated as "Euro 4+" in Table 1. The diesel fuel used for the Honda Accord in both configurations was "low sulfur" (< 10 ppm S) and the lube oil used had a sulfur content of 8900 ppm (wt). The second car used meets the "Euro 3" emission standard and is a 1.8L gasoline Toyota Corolla equipped with a three-way catalytic converter and twin lambda sensors. The Toyota used typical aftertreatment technology for gasoline cars in both Europe and the United States. Unleaded gasoline with a research octane number (RON) of 95 and synthetic lube oil were used in the Toyota. The third vehicle used was an older 1.9L diesel Volkswagen Golf. In its original configuration – with an installed oxidation catalyst – the Golf was "Euro 2" compliant. For the "baseline" configuration reported here, the catalyst was removed to simulate diesel PM emissions with no aftertreatment. The diesel fuel used for the Golf had a nominal sulfur content of 50 ppm (wt) or "Euro 1". The same Golf was also operated using an 100% (neat) soy "biodiesel" with the oxidation catalyst replaced. "Biodiesels" are fuels composted of fatty acid methyl esters (FAME) derived from the esterification of vegetable oils. Biodiesels are alternative fuels, but their use is expected to increase in the future due to both climate change and fuel security concerns. This particular biodiesel (B100) has near-zero sulfur content (2 ppm (wt) S), a mass-based ester content of 96.6%, and a gross heating value of 38 MJ/kg (see Fontaras et al., 2009 for more information on the fuel). Table 2 lists the properties of the fuels used in the Golf. Semi-synthetic lube oil was used in both Golf configurations.

We note that the addition or removal of a control device might lead to changes in engine operation. The exhaust emissions reported in this study were not optimized to the configurations used. The emission rates might be different if the engine and the aftertreatment system is calibrated and optimized in the new configuration.

A schematic of the Constant Volume Sampling (CVS) dilution system used for the collection of the exhaust PM is shown in figure 1. (A more thorough description of the facility and experimental set-up can be found in the literature (Geller et al., 2006, Fontaras et al., 2009).) The exhaust of the tested vehicles was transferred through an insulated 6 m long corrugated stainless steel tube to the CVS dilution tunnel where an orifice forced rapid mixing with the dilution air. A positive displacement pump was using to control the nominal flow rate of the diluted exhaust gas at ca. 600 Nm^3/h through the tunnel. Note the location of the paired quartz and Teflon filters (Q1/T1 and Q2/T2) in the CVS system. (Paired filters of different material (Quartz: Pallflex Tissu Quartz 2500 QAT-UP, Teflon: Pallflex PTFE TX40H120-WW) are used to permit the full chemical analysis of the PM emissions.) The Q1/T1 filters collect the exhaust directly from the CVS system. The Q2/T2 filters were downstream of a versatile aerosol concentration enrichment system (VACES, Kim et al., 2001, Zhao et al., 2005) which was used to concentrate the aerosol from the CVS in order to collect sufficient PM mass for additional analyses. An in-line impinger (BioSampler, SKC West Inc.) was additionally used downstream of the VACES to collect PM in de-ionized water for the toxicity assays. Data from fhe filters downstream of the VACES (e.g. Q2/T2) are not reported herein except to validate the use of the Bio-Sampler (see discussion below). The flow rates reported in figure 1 were confirmed through the use of TSI 4043 flowmeters to within 2%. The analysis of the PM collected on filters and in the impinger during the emissions testing is reported here. The physical properties of the PM (mass concentration, volatility and number concentration) were also measured during the dynamometer tests, but are not reported here.

Each vehicle was driven on a chassis dynamometer over driving cycles designed to cover a range of driving conditions. The measurement protocol, which was the same for every vehicle, consisted of a cold-start New European Driving Cycle (NEDC) and the series of "ARTEMIS" driving cycles. NEDC is four

repeated urban sub-cycles with a maximum speed of 50 km/h and an extra-urban driving sub-cycle (EUDC) with a top speed of 120 km/h. The three ARTEMIS (Andre, 2004) cycles – urban, rural road and motorway – were developed to simulate typical driving conditions in Europe with more frequent variation in vehicle speed and stronger acceleration than in the NEDC. The ARTEMIS cycles more closely simulate real-world driving conditions. All vehicles were also performed a steady-state test at 90 km/h in order to obtain particle size distribution data. Prior to formal emissions testing, each vehicle and sampling system were conditioned by running three EUDC test cycles prior to the actual measurements in accordance with established testing protocols. In order to obtain the cold-start in the actual testing, each vehicle was left for at least 8 hours after conditioning.

Five T1 and five Q1 filter samples (one per cycle) were collected for each "high emitting" vehicle (all the diesel configurations without the DPF). One composite T1 and Q1 filter sample collected across all cycles were collected for the "low-emitting" vehicles (gasoline and DPF-equipped diesel). Each low-emitting vehicle was tested twice and the results combined in order to improve the quantification of the observations.

After sampling, the four filters (Q1, Q2, T1 and T2) were conditioned in a constant humidity (40%) and temperature (22°C) chamber for 24 hours to permit the collected mass to reach equilibrium. The T1 and T2 filters were weighted both before and after sampling using a Mettler-Toledo MX5 microbalance to determine the mass of collected PM. As a quality control step, laboratory filter blanks were also weighed before, during and after each weighing session to verify the accuracy and consistency of the weight measurements.

PM collected on the Q1/T1 filter pair was analyzed for elemental and organic carbon (EC, OC); water-soluble and water-insoluble organic carbon (WSOC, WISOC); inorganic ions (chloride, sulfate, nitrate, phosphate, sodium and ammonium); trace elements and metals, and speciated organic compounds. The aqueous PM suspensions collected by the Bio-Sampler were used in the DTT and ROS toxicity assays.

Extracts from sections of the Teflon substrates are used to determine the concentrations of trace elements and metals, inorganic ions and WSOC of the PM. One extract was analyzed by means of Inductively Coupled Plasma-Mass Spectroscopy (ICP-MS) to determine the particle concentrations of the trace elements and metals. Of particular interest are the concentrations of the following metals: Na, Mg, Al, K, Ca, Ti, V, Cr, Be, S, Mn, Fe, Co, Cu, Zn, Mo, V, Sr, Ba, Cd, Pt, Pb and Ni. These metals were selected because previous inhalation or in vitro studies have shown them to be potentially toxic (Becker et al., 2005, Vogl and Elstner, 1989, among others). The extract from another section of the Teflon filter was analyzed by means of ion chromatography (IC) for sulfate, nitrate, sodium, potassium and ammonium ions ($SO_4^=$, NO_3^-, Na^+, K^+, NH_4^+). Lough et al. (2005) describe in detail the procedures followed for the sample processing (e.g. filter/substrate extraction methods, digestion) in the IC and ICP-MS analyses. The IC analysis used a modified version of the NIOSH (National Institute for Occupational Safety and Health) Method 7903 and OSHA (Occupational Safety and Health Administration) Method 188. Another section of the Teflon substrate was analyzed for WSOC using a Sievers Total Organic Carbon analyzer (General Electric, Inc.) (Zhang et al., 2008). The quartz substrates were also sectioned prior to analysis. One quartz filter section was analyzed for elemental carbon (EC) and organic carbon (OC) concentrations. These analyses were conducted according to the NIOSH Thermal Desorption/Optical Transmission method (Birch and Carey, 1996). Extracts from the quartz filter substrates were also used for the organic compound speciation analysis that focuses on PAHs, phthalates, pesticides and total WSOC (Sheesley, 2004). The organic species, including polycyclic aromatic hydrocarbon (PAHs), hopanes, steranes, n-alkanes and organic acids, were quantified by gas chromatography/mass spectrometry (GC/MS) (Stone et al. 2008). All Teflon and quartz filter samples were stored in –20°C freezers.

As mentioned above, the two toxicity assays were conducted on the liquid PM suspension. The dithiothreitol (DTT) assay provides a measure of the overall redox activity of a given sample based upon its ability to catalyze electron transfer between DTT and oxygen in a simple chemical system (Cho et al., 2005). It is sensitive to the redox activity of organic compounds and is particularly appropriate for motor vehicle exhaust. The electron transfer is monitored by the rate at which DTT is consumed under a

standardized set of conditions. The rate is proportional to the concentration of the catalytically-active, redox-active species in the sample. The data collected at the multiple time points are used to determine the rate of DTT consumption for the sample.

The redox activity/ROS production of exhaust emission PM was also measured using a biological ROS assay in addition to the DTT test.   The biological assay involves in vitro exposure to rat alveolar macrophage (AM) cells using dichlorofluorescin diacetate (DCFH-DA) as the fluorescent probe and examines the production of ROS as well as the response of AM cells. Alveolar macrophages from the NR8383 cell lines (American Type Culture Collection) were exposed to aqueous suspensions of PM and subsequently assessed for viability (membrane integrity) and production of ROS as an indicator of macrophage stimulation using the methods developed by Landreman and colleagues at the University of Wisconsin (Landreman et al., 2008). Samples were extracted with purified water and then filtered through a 0.22 µm pore size filter to isolate the water-soluble and colloidal fraction of the sample. The sample extracts were then buffered in a salt and glucose medium and subsequently split to prepare aliquots of diluted and non-diluted samples for cell exposures in triplicate. Zymosan (a β-1,3 polysaccharide of D-glucose) was chosen as the primary positive control because it is recognized by the TLR-2 receptors on macrophage cells, activating a strong immuno-chemical response. Following incubation at 37°C for two hours, the fluorescent intensity was measured using a Cytoflour II automated fluorescence plate reader. All results are reported in units of Zymonsan equivalents given the positive control used. This ROS assay has been previously used to characterize a wide range of aerosol samples including atmospheric particulate matter samples from Denver (Zhang et al. 2008) and Los Angeles (Hu et al. 2008), as well as atmospheric aerosol samples impacted by large forest fires (Verma et al. 2009).

Where appropriate (see the Appendix) the chemical composition and toxicological assay results were blank-corrected using tunnel blanks. Tunnel blank subtracted values ≤ 0 were reported as below detection limit (BDL), and were interpreted as zeros in all calculations and correlations. Tunnel blank-subtracted values that are larger than zero are reported with uncertainties. A limit of detection (LOD) table

is provided in the Appendix for reference; and the detection limit is defined as 3 times the analytical uncertainty of the tunnel blanks obtained during this study.

Results and Discussion

PM mass emission rates (mg/km) are reported first followed by the chemical composition of the exhaust emissions. Emission factors for all species are then presented followed by the toxicity assay results. Correlations among and between the chemical composition of the PM and the PM's oxidative potential are then shown.

PM Mass Emissions

Mass emission rates (mg/km) for PM and selected chemical species (OC, EC, WSOC, nitrate, sulfate, ammonium and sum of inorganic ions) derived from the Q1/T1 filter pair are shown in Table 3. The values shown are calculated based upon the entire driving cycle. The reconstructed mass for these filters based upon the reported chemical composition (including EC, OM (organic material) and inorganic ions) agrees well with the gravimetric mass (both expressed in terms of mg/km) (figure 2). In this reconstruction, OM was calculated by multiplying a factor of 1.43, 1.55 and 1.34 times the OC results for the Accord, Corolla and Golf vehicles, respectively. These factors were calculated based upon the relative WSOC vs WISOC contributions to OC in each vehicle (see Turpin et al., 2001). Measured and reconstructed mass agree very well with each other (within 10%) and are highly correlated (slope = 0.99, r^2 = 0.99). Unsurprisingly, the baseline Golf diesel vehicle at the oldest emission control standard had the highest emission rates. The other two non-DPF equipped diesel and biodiesel-fuelled vehicles also had high emission rates. The DPF-equipped diesel and the gasoline vehicle had substantially lower PM mass emission rates. The DPF-equipped diesel had the lowest overall mass emission rates indicating the effectiveness of the DPF.

Chemical Composition

The relative contribution of each chemical species to the total emission rate for each vehicle is shown in figure 3. Again it was necessary to convert WSOC and WISOC to water soluble organic matter (WSOM) and water soluble insoluble organic matter (WISOM), respectively using factors of 2 and 1.3 (Turpin et al., 2001). Elemental Carbon contributed the highest PM fraction to the Accord and the baseline Golf diesel vehicles (73 and 55%, respectively). The biodiesel Golf had substantially lower EC concentrations (15%). This suggests that the additional oxygen atoms present due to the esterification process in the biodiesel minimize soot formation and promote oxidation. The DPF equipment on the Accord removed EC effectively. Beyond the EC concentrations, the additional species measured varied considerably among the five configurations tested. For the gasoline vehicle, inorganic ions formed more than 50% of the mass but were negligible for the baseline diesel vehicle.

Emission Factors: Organic Carbon (OC) and Elemental Carbon (EC)

The Accord diesel, the Golf diesel and the Golf biodiesel emitted sufficient PM that a detailed analysis of the emission factors for each driving cycle was possible (in contrast, insufficient PM emissions by the DPF-equipped Accord diesel and the Corolla gasoline vehicle allowed the determination of only a single emission factor across all driving cycles). OC and EC emission data (mg/km) for each vehicle is shown in figure 4. For the three high emitters, steady-state emissions were ca. 25 – 30% and 65% lower than for the other driving cycles for OC and EC, respectively. The non-DPF equipped diesels all have higher OC and EC emission rates than the gasoline vehicle. Use of the DPF reduced OC and EC emissions by 90 and 99%, respectively. While the DPF mostly captures non-volatile soot particles, the significant reduction in tailpipe PM lowers the aerosol surface area available for the condensation of semi-volatile organic vapors. The particulate OC concentrations in the exhaust are also reduced. Further, the DPF may also participate in the oxidation of OC vapors which may present a second mechanism to reduce OC particulate concentrations in the exhaust.

Using the biodiesel fuel reduced EC emissions and the relative contribution of EC to total carbon (TC, TC = OC + EC) by 70 – 85% across the different driving cycles. As described above, the additional presence of oxygen in the fuel should inhibit in-cylinder soot production. However, OC emissions for the baseline and biodiesel Golf were very similar across all driving cycles, regardless of the use of the oxidation catalyst for the latter. In view of the composition of the fuel with corresponding changes in combustion conditions within the engine (Fontaras et al., 2009), higher OC emission factors should be produced by the biodiesel Golf but, in this instance, appear to have been counterbalanced by the addition of the oxidation catalyst.

The Accord diesel, the Golf diesel and the Golf biodiesel vehicles emitted similar levels of WSOC (0.91 – 1.48 mg/km). The DPF-equipped Accord and the Corolla gasoline vehicle has significantly lower emission factors for EC, WSOC and WISOC than the high emitters by factors of up to ca. 10). An earlier study of baseline heavy-duty diesel vehicles compared to ones with retrofitted control technology indicated that WSOC/OC ratios were lower in the baseline vehicles (Biswas et al., 2009). The light-duty results reported here are consistent with these results – the baseline Golf diesel vehicle had a low WSOC/OC ratio (ca. 0.06) and the newer Accord in both configurations showed higher relative OC solubility (ca. 0.19 with and without the DPF).

Emission Factors: Speciated Organic Compounds

Table 4 shows the emission factors for polycyclic aromatic hydrocarbons (PAHs), hopanes, steranes, alkanes, and organic acids (OA). PAHs are subdivided into three categories according to their molecular weights (MW): MW ≤ 228 [Phenanthrene, anthracene, fluoranthene, acephenanthrylene, pyrene, methylfluoranthene, benzo(GHI)fluoranthene, cyclopenta(cd)pyrene, benz(a)anthracene, chrysene], MW = 252 [Benzo(b)fluoranthene, benzo(k)fluoranthene, benzo(j)fluoranthene, benzo(e)pyrene and benzo(a)pyrene] and MW ≥ 276 [Indeno (1,2,3-cd)pyrene, benzo(ghi)perylene, dibenz(ah)anthracene, picene, coronene, and dibenzo(ae)pyrene]. The Golf petrodiesel vehicle with no aftertreatment emitted the highest amount of PAHs and the Golf with the biodiesel configuration emitted the second highest

amounts. The gasoline Corolla emitted higher proportions of the heavy PAHs (MW ≥ 276) compared to the petrodiesel vehicles, which is consistent with earlier studies (Miguel et al. 1998; Zielinska et al. 2004). Heavier MW PAHs are emitted only from the gasoline and biodiesel cars. Similarly to total PAHs, light MW PAH (MW ≤ 228) emissions were highest from the Golf petrodiesel vehicle, followed by the Golf biodiesel and the Accord diesel. Biodiesel emissions of light MW PAHs, however, were approximately 50% lower compared to the original (petrodiesel) configuration. Recent studies have reported similar observations (Correa and Arbilla 2006; Chien et al. 2009). The reduction in light PAH emission factors may be attributable to the properties of the soybean biodiesel. Unlike petrodiesel, this fuel has very little or negligible aromatic content (see Table 2). Light MW PAHs are important in terms of the potential to generate oxidative stress (Li et al. 2003). As discussed elsewhere, the relatively high oxygen content due to esterification of the fuel and the presence of the oxidation catalyst may have also facilitated PAH oxidation. Biodiesel contains unsaturated components and results in higher flame temperatures than petro-diesel, providing favorable conditions for the formation of larger PAH molecules (Jha et al. 2008). The different PAH profiles of the biodiesel and petrodiesel Golf configurations also suggests that the combustion chemistry may be markedly different in the two systems.

While heavier MW PAHs are typically present in the particle phase, the light MW semi-volatile PAHs partition between the gas and particle phases. The DPF-equipped Accord configuration removed the semi-volatile PAHs to levels below their detection limits (see the Appendix). These values are much lower than emissions from the Accord in its original configuration, highlighting the effectiveness of the DPF from the toxicological perspective. The petrodiesel Golf emitted the highest amounts of semi-volatile PAHs compared with the other two vehicles. While the semi-volatile PAHs emissions of the biodiesel vehicle was decreased by 50% (see above) compared to its baseline petrodiesel configuration, the sum of the semi-volatil PAHs from the biodiesel car (7.76 µg/km) is still much higher than the Accord diesel (2.55 µg/km), the DPF-Accord (BDL) and the gasoline vehicle (0.20 µg/km).

Figure 5 shows 12 of the 16 U.S. EPA priority PAHs identified in this study of which 7 are probable human carcinogens. The results observed for these PAHs are consistent with the results discussed

above for the different MW PAH fractions. The baseline petrodiesel Golf emitted the highest total sum of these 12 PAHs (13.9 µg/km), followed by the biodiesel Golf (8.54 µg/km) and the Accord diesel (2.55 µg/km). The DPF-equipped Accord diesel vehicle removed the 12 PAHs to levels below their detection limits due to the effectiveness of the DPF. The petrodiesel Golf emitted 4 out of the 7 probable carcinogenic PAHs at factors ranging from 128 to 1180 ng/km. The biodiesel Golf emitted two more probable carcinogens but overall concentration factors were reduced (individual species varied from 154 to 609 ng/km). The gasoline Corolla emitted a considerable amount of carcinogenic PAHs, but its calculated emission factors remained lower than those derived for the Golf in both configurations. These results suggest that the use of efficient emission control technologies (such as DPF) or cleaner fuel (gasoline) may be far more effective in reducing the emissions of carcinogenic substances like PAHs than the use of biodiesel.

Figure 6 shows the emission factors of individual hopanes and steranes. Hopanes and steranes originate from the lube oil and are widely used as tracers of vehicular emissions (Rogge et al. 1993; Fraser et al. 1999). The Golf in both configurations emitted the highest hopane and sterane emissions compared to the other diesel vehicles. Although the biodiesel configuration was equipped with an oxidation catalyst, it did not effectively remove any hopanes and steranes. Further, the obvious similarity in the emission factors and profiles of hopanes and steranes suggests that they were exclusively from lube oil, since these two vehicle configurations used different fuel (petro-diesel and biodiesel) but the same lube oil. When the emission factors (µg/km) of the hopanes are normalized to total carbon (OC+EC) (mg/km), the ratios are 1073 and 1911 µg/g for the Golf diesel and Golf biodiesel vehicles, respectively. The difference might be attributable to the much lower EC levels in the biodiesel configuration. The DPF-Accord vehicle, on the other hand, yielded high reductions of hopanes and steranes compared to its original configuration. The DPF reduced 4 of the 7 hopanes to concentration levels below their limits of detection. The Accord diesel and the gasoline vehicle did not emit detectable amounts of steranes. This may be important in future studies. As steranes are often used as tracers of vehicle exhaust; non-detectable emissions by cleaner and newer vehicles might impact modeling efforts in source apportionment studies.

Alkanes are species that may originate from diesel fuel as well as unburned oil. High alkane emission factors are again observed for the baseline Golf petrodiesel followed by the Accord diesel. Figure 7 shows the emission factors of speciated alkanes for each vehicle configuration. The Golf petrodiesel emitted high levels of nonadecane, eicosane, heneicosane and docosane (ranging from 139 to 215 µg/km). The newer Accord diesel vehicle had overall lower alkane emissions, but emitted a more diverse profile of these species than the Golf using the same fuel. In contrast, alkane levels were low in the biodiesel vehicle since this type of biodiesel does not contain alkanes. This is an important consideration for source apportionment modeling for fleets with a high proportion of biodiesel vehicles.

Figure 8 shows the emission factors of organic acids detected in this study. Hexadecanoic acid, octadecanoic acid, oleic acid, linoleic acid and linolenic acid are ingredients of soybean biodiesel (Kincs 1985). High emission factors for hexadecanoic, octadecanoic, oleic and linoleic acids are observed from the Golf biodiesel, consistent with the fuel's reported components and any possible incomplete combustion. Furthermore, the biodiesel fuel used in the study is composed of methyl esters produced from soybeans. During combustion, these methyl esters may demethylate at high temperatures (Knothe 2006). The biodiesel used in this study had a low stability due to its high linolenic acid ester (5.8%) content. Since the analyses of the fatty acids were done by converting these acids to methyl esters, the high emissions of these acids are expected to originate from the esters, as well as the acids formed during demethylation. Linolenic acid was not detectable in the biodiesel Golf's emissions. Linolenic acid, however, is an unstable compound with three double bonds, in contrast to the other acids which are much more stable. Therefore its absence may be a sampling artifact.

As described above, the DPF employed in this study was a platinum coated silicon carbide filter of octagonal channel cross-section with a cell density of 300 cells/in^2. The platinum coating acts as a media for catalytic oxidation. Figure 9 shows the DPF-equipped Accord's removal rates for selected elements, PAHs, elemental carbon, organic carbon and water soluble organic carbon (S and Fe are not included in figure 9 since they were relatively elevated in this configuration). (The emission factors for trace elements and metals are discussed in additional detail below.) Elevated sulfur concentrations were probably due to

nucleation following the filter as discussed earlier. Fe, on the other hand, was present in trace levels with high uncertainties. Cu is excluded due to the low levels observed and the associated uncertainties. Overall, Figure 9 shows lower removal efficiency for certain elements (35, 51, 71 and 80% for Ni, Co, Mn and Cr, respectively). Part of this lower removal efficiency may be due to analytical uncertainties associated with the already low emission levels of some of these trace elements.

The DPF removed much higher relative amounts of PAHs than trace elements (down to below the detection limits). Meanwhile, only 90% of the organic carbon was removed. Since the DPF in the Accord vehicle also acted as a catalyst, the differential removal efficiency for OC and the PAHs might be due to a combined filtering/catalytic activity. The high removal rate of PAHs confirms the effectiveness of the DPF in reducing carcinogenic compounds, which is clearly one of the major benefits of introducing this type of an aftertreatment technology.

Emission Factors: Inorganic Ions

The emission factors for inorganic ions are shown in figure 10. The Golf biodiesel was the highest overall emitter of inorganic species. Despite the low overall mass emission levels, the gasoline Corolla also had high emission factors for these species. Interestingly, the sulfate emission factor was highest for the gasoline vehicle due to the very low sulfur diesel fuels used. The relatively high sulfate emission factor for the biodiesel vehicle is likely due to the sulfur in the lube oil as there is virtually no S in the biodiesel itself. This suggests that the sulfur content of lube oils has the potential to be important in S emissions associated with motor vehicles.

Ammonium emissions from the gasoline vehicle were 12 – 20 times higher than from the diesel vehicles. This is consistent with previous observations of high ammonium emission factors associated with reactions induced by the presence of the three-way catalytic converter (Heeb et al., 2006, Kean et al., 2009). Light-duty diesel vehicles, as a result, are a relatively minor source of ammonium ion. The petrodiesel and biodiesel Golf inorganic nitrogen emission factors vary. The highest nitrate emission

factor from the biodiesel is consistent with earlier work investigating biodiesel emissions (Fontaras et al., 2009) as well as the presence of the oxidation catalyst. The presence of the catalyst may in part account for the relatively lower ammonium emission factor from the biodiesel compared to the petrodiesel.

Emission Factors: Trace Elements and Metals

Table 5 lists emission factors of: selected trace elements and metals. Crustal elements are shown at the top of the Table 5 because their contributions to elemental emissions are higher than anthropogenic elements in diesel vehicles (Wang et al. 2003). In summary, the Golf petrodiesel and biodiesel vehicles were characterized by the highest PM mass emissions. The DPF-equipped diesel vehicle reduced 98% of the mass emissions compared to its original configuration, and to a lower level than the gasoline car.

Sulfur emissions were highest among the non-metallic elements in each vehicle configuration. The high sulfur emission observed in the gasoline vehicle is consistent with the inorganic ions data, which showed high sulfate ion emissions. Sulfate emission (0.99 mg/km) was about 3.2 times that of sulfur (0.30 mg/km), very close to the molecular weight ratio of sulfate to sulfur, suggesting that most of the sulfur come from sulfates. When compared with the Golf diesel vehicle, which used fuel with the same sulfur content and lube oil with different sulfur content, the gasoline car yielded higher sulfur emissions. The diesel vehicle used a lubrication oil of 8900 ppm S, while the respective value for the oil used in the gasoline vehicle was 5000 ppm. Since the historical lubricant oil consumption records we have for the two cars (~50 ml/1000 km) do not provide evidence of higher consumption of the gasoline than the diesel vehicle, the high sulfate emissions in the gasoline car must be due to the formation of sulfate nanoparticles through nucleation processes occurringdownstream of the 3-way catalytic converter. On the other hand, gasoline cars do not usually produce high sulfate levels because there is no oxygen surplus in the exhaust to oxidize sulfur. This particular gasoline vehicle, however, was equipped with secondary air injection, i.e. a small quantity of secondary air (SAI) is injected into the exhaust when required to oxidize hydrocarbons and carbon monoxide. This SAI may result in high sulfate formation as it provides the missing oxygen to form sulfates. The gasoline vehicle was also characterized by higher emissions of

Mn, Fe and Cu compared with the DPF-Accord vehicle, consistent with previous studies (Geller et al. 2006). Mn is a known knock improver; it was probably used in the gasoline car at trace concentration levels in order to improve the octane number of the fuel.

Despite the high emission reductions of most inorganic ions, the Accord vehicle shows a 26% increase in sulfur emissions when equipped with the DPF. Several earlier studies showed that particle nucleation in diesel vehicles occurs following the after-treatment devices (Vaaraslahti et al. 2004; Kittelson et al. 2006; Biswas et al. 2009b). For example, Vaaraslahti et al showed formation of new particles occurred downstream of the DPF and suggested that sulfuric acid was the main nucleating species (Vaaraslahti et al. 2004). Biswas et al (2009b) showed that the formation of fresh nano-particles via nucleation in DPF-equipped diesel trucks was attributed to a ternary nucleation process involving sulfuric acid, water vapor and ammonia. These observations are consistent with our study. Sulfur emissions are similar between the two configurations (petro-diesel or biodiesel) of Golf vehicle, which used the same lube oil, suggesting that a significant fraction of sulfur in these vehicles may be originating from lube oil. The diesel vehicle (Golf) used a fuel with a 50 ppm S content, and without any after-treatment technology, particulate sulfur could be contributed by both the fuel and the lube oil. But its sulfur emission (81.4 µg/km) is relatively low considering the high sulfur content in its fuel. Thus, it is believed that most of the sulfur was converted to SO_2 and released as a gas. Although the biodiesel vehicle had less sulfur in its fuel, its oxidation catalyst may counterbalance the reduced sulfur by oxidizing any trace sulfur in the fuel and the lube oil.

Potassium and sodium emissions were higher in the biodiesel vehicle compared to the same vehicle operating with diesel by factors of 39 and 6, respectively. The increased emissions of these species may be due to the fact that KOH and NaOH were used as catalysts in the esterification process. These compounds probably remained in the biodiesel and were subsequently emitted as particles.

Correlations among PM Species

Table 6 presents correlations among the PM chemical species analyzed. Values with correlation coefficients > 0.80 and p < 0.05 are in bold. Results of Cu, heavy PAHs (MW≥ 276) and steranes are not included, as only 2 out of 5 data points have detectable values. Zn, P and Ca are highly correlated (r >0.84) and are all significant ingredients of lube oil. Zn and P are present in lube oil as zinc dithiophosphate, an antioxidant and anti-wear compound. The high correlations suggest that these species mostly originate from lube oil, irrespective of fuel and aftertreatment technology used. The high correlations (r >0.88) of these elements (Zn, P and Ca) with hopanes further confirm this hypothesis. Furthermore, Na and K are well-correlated with organic acids (r =0.99 and 1.0 respectively) as they are derived from the biodiesel.

Oxidative Potential from Different Vehicles and Configurations

The DTT consumption rates are shown both on a per PM mass [nmol/(min x μg)] and a per km driven [nmol/(min x km)] basis for each vehicle configuration (Table 7). The non-DPF equipped Accord and the biodiesel Golf have the most potent exhausts on a per PM mass basis. However, the per km oxidative activity of the biodiesel (1040 ± 124 nmol/(min-km)) is almost double that for the Accord (624 ± 54 nmol/(min-km)) because of the relatively lower mass emission rate. Not surprisingly, the DTT consumption rate of the petrodiesel Golf (expressed on a per km driven basis) was the highest of all the configurations studied (1300 ± 216 nmol/(mol-km))because it had the highest PM emission rate and high concentrations of other oxidative-active species such as OC, EC and WSOC. While the use of the biodiesel and the oxidation catalyst reduced the biodiesel Golf's PM mass emissions by 43% (from ca. 72 to 41 mg/km), the corresponding decrease in oxidative potential was only ca. 20%. This may be due to the relatively similar OC emission factors for both Golf configurations (24.2 and 24.4 mg/km for the petrodiesel and biodiesel, respectively). The use of the DPF on the Accord diesel produced the lowest oxidative activity per km (12.0 ±1.3 nmol/(min-km)). This suggests that the DPF technology is also effective at reducing the toxicological impact of diesel emissions on human exposure. The oxidative activity of the DPF-equipped diesel was fully 60% lower than that for the gasoline vehicle – also characterized by a low oxidative activity rate – because of its comparatively lower mass emission rate.

The results of the macrophage-ROS assays also used to assess the oxidative potential of PM samples are shown in Table 8 expressed in units of distance driven. The macrophage ROS assay is sensitive to transition metals because of their ability to catalyze redox-reactions in which they are not consumed. The per km-based ROS response provides the actual toxicological activity imparted on the environment and humans by these vehicles. The ROS activity, expressed in μg of Zymosan units/km, is highest for the gasoline vehicle despite its relatively low mass emissions. This is due to its higher elemental content compared to the other four configurations. The Accord vehicle, in contrast, demonstrates non-detectable ROS-measured activity in both configurations (with or without the DPF).

Correlations between Chemical Constituents and toxicological assays

Correlations between the DTT consumption rates and the chemical constituents were used to asses the toxicological contribution of each chemical species. The PM suspension used for the DTT assay was collected downstream of the VACES (see figure 1). Therefore in order to compare these two sets of results, the performance of the VACES must be assessed. The comparison between the PM masses reconstructed from the chemical composition both upstream and downstream of the VACES is shown in Figure 11. The upstream reconstruction assumed the theoretical concentration enrichment factor for the operating conditions used. Overall, the comparison of the reconstructed mass emission rates is reasonably good (slope = 1.13, r^2 = 0.79). Therefore the use of data collected both upstream and downstream of the VACES in the dilution system is valid.

The correlation plots between DTT consumption rates and various chemical species in the PM are shown in figure 12. Given the assay, it is not surprising that good correlation is found between carbonaceous species (EC, WSOC, WISOC and OC) and the DTT consumption rate. There is no correlation between inorganic ion emission rates and DTT consumption rate as we have previously observed in other studies (Ntziachristos et al., 2007). Pearson correlation coefficients (r), corresponding significance levels (p), regression slopes, and y-intercepts are shown in Table 9. The DTT consumption rate based upon the

distance drive was best correlated with WSOC (r = 0.98, p < 0.01) which is also consistent with earlier studies (Geller et al., 2006, among others). The regression slope for WSOC is also much higher than observed for the other species indicating its impact.

Correlations between ROS activity (μg of Zymosan units/km), DTT consumption rates [nmol/(min-km)] and selected trace elements (ng/km) were used to assess the toxicological contribution of these species to each of these assays. Results shown in Table 10 indicate that ROS is strongly correlated with soluble Fe (r =0.99, p <0.01); other elements such as S and Mn also have correlations (r =0.77 and 0.79, respectively) that approach statistical significance. Valavanidis et al. (2000) measured the generation of hydroxyl radicals and indicated that oxidant generating activity is related to soluble iron ion concentrations. Since the measured ROS probe used in this method is sensitive to $HO^{.}$ and H_2O_2 (Schoonen et al. 2006), the high correlation of Fe to ROS is consistent with these previous findings (Valavanidis et al. 2000). Another study by Aust et al. (2002) evaluated the potential generation of ROS from vehicular PM by measuring the formation of malondialdehyde, and concluded that most ROS activity was caused by soluble iron, which is also consistent with the findings presented here (Aust et al. 2002). To a certain degree the ROS associations with other elements may be confounded by the modest association of Fe with these species, as most of these are ingredients of lube oil (this includes the moderate correlation of Fe with hopanes). Fe is not highly correlated, however, with any other organic and inorganic species (Table 6), and therefore its presence in the exhaust may be due to factors other than lube oil, such as engine wear. Ni and V are not correlated with ROS in this study, in contrast to previous studies (Verma et al. 2009). This is probably due to the low emission factors observed for these species in this study (<50 ng/km for V and <7 ng/km for Ni) as vehicles of this type are not the primary sources for these species in urban environments (Cass and McRae, 1983). P, Zn and Ba appear to have high and significant correlations with DTT consistent with their elevated presence in lube oil. Here again, this high correlation may be confounded due to the high levels of organic species in lube oil that at least mechanistically influence the DTT-measured oxidative activity.

In addition to the relationship between oxidative potential and the more general OC and EC compound classes, correlations between DTT consumption rates, ROS activity and selected organic compounds exist (Table 11). As discussed earlier, organic compounds are the major species driving DTT consumption rates, consistent with many earlier studies (Cho et al. 2005; Ntziachristos et al. 2007; Biswas et al. 2009a). Correlation results for the heavy PAHs (MW ≥ 276) and steranes are not included, as only two of the five data points have detectable values. The correlation analysis indicates that DTT rates are strongly correlated with the following species: Sum of PAHs (r=0.94), lighter MW PAHs (r=0.93), and hopanes (r=0.91). Since heavier PAHs (MW=252) are water insoluble, they are less correlated with DTT. The high emissions of organic acids (OA) from biodiesel do not seem to affect the DTT consumption rate. PAHs and hopanes have moderate correlations with ROS although none of these reach significance. ROS and DTT are not correlated with each other due to the different development of oxidative stress in each method.

Conclusions

Our results have shown lower emissions and distance-based oxidative potential for the DPF-equipped diesel and gasoline vehicles. Diesel and biodiesel vehicles had the highest PM emission rates and the most toxicologically-potent exhaust in terms of oxidative potential (as measured by the DTT and macrophage ROS assays). The distance-based oxidative activity is strongly associated with the WSOC content of the exhaust and, to a lesser extent, with OC and WISOC. More specifically, the Golf diesel in either configuration had the highest emissions of organic species (PAHs, hopanes, steranes and organic acids). The biodiesel Golf had relatively elevated emissions of several organic acids but this did not appear to affect the oxidative properties of the emitted PM. The DPF-equipped Accord diesel car, by comparison, was effective in reducing overall PAHs and PM mass, and had the least potent emissions measured by both DTT and ROS assays. Thus, to reduce the emissions of carcinogenic aromatics, the use of advance aftertreatment technologies and/or cleaner fuel may be a better remedy than the use of biodiesel. Our results indicated that soluble Fe is highly correlated with particulate ROS activity (r =0.99), while PAHs and hopanes are highly correlated with the DTT consumption rates (r =0.94 and 0.91,

respectively). The DTT-measured PM activity was found to be strongly associated with tracers of lube oil emissions, such as Zn, P, Ca and hopanes (r =0.96, 0.92, 0.83 and 0.91 respectively), suggesting that incomplete combustion of lube oil plays a significant role in the overall PM-induced oxidative potential of vehicular exhaust.

Students supported

Two Ph.D. students in Dr. Sioutas' group at USC were supported by METRANS through funding for this project: Mohammed Arhami and Ka Lam Cheung. Dr. Arhami defended his doctoral dissertation in January 2009 and recently received a faculty appointment to Sharif University of Technology (Tehran, Iran).

Project Publications

The results from this METRANS project have been reported to the scientific community in two manuscripts:

Cheung, KL; Polidori, A; Ntziachristos, L; Tzamkiozis, T; Samaras, Z; Cassee, FR, Gerlofs, M and C Sioutas (2009). Chemical characteristics and oxidative potential of particulate matter emissions from gasoline, diesel, and biodiesel cars. *Environmental Science and Technology*, **43**(16), 6334 – 6340. doi:10.102/es900819t

Cheung, KL; Ntziachristos, L; Tzamkiozis; Schauer, JJ; Samaras, Z; Moore, KF and C Sioutas (2009). Emissions of particulate trace elements, metals and organic species from gasoline, diesel and biodiesel passenger vehicles and their relation to oxidative potential. *in review, Aerosol Science and Technology (submitted August 2009).*

The ISI Web of Knowledge impact factors are 4.458 and 2.268 for Environmental Science and Technology and Aerosol Science and Technology, respectively. These are both highly cited and well-regarded journals in the community.

These results have also been presented by the authors at multiple national and international scientific conferences including the annual meeting of the American Association of Aerosol Research.

References

Andre, M (2004). The ARTEMIS European driving cycles for measuring car pollutant emissions. *Science of the Total Environment*, **334/5**, 73 – 84.

Aust, A. E., Ball, J. C., Hu, A. A., Lighty, J. S., Smith, K. R., Straccia, A. M., Veranth, J. M. and Young, W. C. (2002). Particle characteristics responsible for effects on human lung epithelial cells. *Research report (Health Effects Institute)*:1-65; discussion 67-76.

Bagley, ST, Gratz LD, Johnson, JH and JF McDonald (1998). Effects of an oxidation catalytic converter and a biodiesel fuel on the chemical, mutagenic, and particle size characteristics of emissions from an IDI diesel engine. *Environmental Science and Technology*, **32**, 1183 – 1191.

Becker, S Dailey, LA, Soukup, JM, Grambow, SD, Devlin, RB and YCT Huang (2005). Seasonal variations in air pollution particle-induced inflammatory mediator release and oxidative stress. *Environmental Health Perspectives*, **113(8)**, 1032 – 1038.

Birch, ME and RA Cary (1996). Elemental carbon-based method for monitoring occupational exposures to particulate diesel exhaust. *Aerosol Science and Technology*, **25(3)**, 221 – 241.

Biswas, S, Hu, S, Verma, V, Herner, JD, Robertson, WH, Ayala, A and C Sioutas (2008). Physical properties of particulate matter (PM) from late model heavy duty diesel vehicles operating with advanced PM and NOx emission control technologies. *Atmospheric Environment, in press.*

Biswas, S., Verma, V., Schauer, J. J., Cassee, F. R., Cho, A. K. and Sioutas, C. (2009a). Oxidative Potential of Semi-Volatile and Non Volatile Particulate Matter (PM) from Heavy-Duty Vehicles Retrofitted with Emission Control Technologies. *Environ Sci Technol* 43:3905-3912.

Biswas, S, Verma, V, Schauer, JJ and C Sioutas (2009b). Chemical speciation of PM emissions from heavy duty diesel vehicles equipped with diesel particulate filters and SCR retrofits. *Atmospheric Environment*, **43**, 1917 – 1925.

Cass, G. R. and McRae, G. J. (1983). Source Receptor Reconciliation of Routine Air Monitoring Data for Trace-Metals - an Emission Inventory Assisted Approach. *Environ Sci Technol* 17:129-139.

Chien, S.-M., Huang, Y.-J., Chuang, S.-C. and Yang, H.-H. (2009). Effects of Biodiesel Blending on Particulate and Polycyclic Aromatic Hydrocarbon Emissions in Nano/Ultrafine/Fine/Coarse Ranges from Diesel Engine. *Aerosol and Air Quality Research* 9:19-31.

Cho, AK, Sioutas, C, Miguel, AH, Kumagai, Y, Schmitz, DA, Singh, M, Eiguren-Fernandez, A and JR Froines (2005). Redox activity of airborne particulate matter at different sites in the Los Angeles Basin *Environmental Research*, **99**(1), 40-47.

Correa, S. M. and Arbilla, G. (2006). Aromatic hydrocarbons emissions in diesel and biodiesel exhaust. *Atmospheric Environment* 40:6821-6826.

Delfino, RJ, Sioutas, C and S Malik (2005). Potential role of ultrafine particles in associations between airborne particle mass and cardiovascular health. *Environmental Health Perspectives*, **113(8)**, 934 – 946.

Dockery, DW and CA Pope (2006). Health effects of fine particulate air pollution: lines that connect. *Journal of the Air and Waste Management Association*, **54**, 709 – 742.

Fontaras, GK, Kousoulidou, M, Tzamkiozis, Th, Ntziachristos L and E Bakeas (2009). Effects of biodiesel on passenger car fuel consumption, regulated and non-regulated pollutant emissions over legislated and real world driving cycles. *Fuel, in press.*

Fraser, M. P., Cass, G. R. and Simoneit, B. R. T. (1999). Particulate organic compounds emitted from motor vehicle exhaust and in the urban atmosphere. *Atmospheric Environment* 33:2715-2724.

Gauderman, WJ, Vora, J, McConnell, R, Berhane, K, Gilliland, F, Thomas, D, Lurmann, F, Avol, E, Kunzli, N, Jerrett, M and J Peters (2007). Effect of exposure to traffic on lung development from 10 to 18 years of age: a cohort study. *Lancet*, **369**, 571 – 577.

Geller, MD, Ntziachristos, L, Mamakos, A, Samaras, Z, Schmitz, DA, Froines, JR and C Sioutas (2006). Physicochemical and redox characteristics of particulate matter (PM) emitted from gasoline and diesel passenger cars. *Atmospheric Environment*, **40**, 6988 – 7004.

Grose, M, Sakurai, H, Savstrom, J, Stolzenburg, MR, Watts, WF, Morgan, CG, Murray, IP, Twigg, MV, Kittelson, DB and PH McMurry (2006). Chemical and physical properties of ultrafine diesel exhaust particles sampled downstream of a catalytic trap. *Environmental Science and Technology*, **40**, 5502 – 5507.

Heeb, NV, Forss, AM, Bruhlmann, S, Luscher, R, Saxer, CJ and P Hug (2006). Three-way catalyst-induced formation of ammonia – velocity- and acceleration-dependent emission factors. *Atmospheric Environment*, **40(31)**, 5986 – 5997.

Hu, S., Polidori, A., Arhami, M., Shafer, M. M., Schauer, J. J., Cho, A. and Sioutas, C. (2008). Redox activity and chemical speciation of size fractioned PM in the communities of the Los Angeles-Long Beach harbor. *Atmos Chem Phys* 8:6439-6451.

Jha, S. K., Fernando, S. and To, S. D. H. (2008). Flame temperature analysis of biodiesel blends and components. *Fuel* 87:1982-1988.

Kean, AJ, Ban-Weiss, GA, Harley, RA, Kirchstetter, TW and MM Lunden (2009). Trends in on-road vehicle emissions of ammonia. *Atmospheric Environment*, **43**, 1565 – 1570.

Kim, S, Shen, S and C Sioutas (2002). Size distribution and diurnal and seasonal trends of ultrafine particles in source and receptor sites of the Los Angeles basin. *Journal of the Air and Waste Management Association*, **52**, 297 – 307.

Kim, S, Jacques, PA, Chang, MC, Barone, T, Xiong, C, Friedlander, SK and C Sioutas (2001). Versatile aerosol concentration enrichment system (VACES) for simultaneous in vivo and in vitro evaluation of toxic effects of ultrafine, fine and coarse ambient particles – Part II: Field Evaluation. *Journal of Aerosol Science*, **32(11)**, 1299 – 1314.

Kincs, F. R. (1985). Meat Fat Formulation. *J Am Oil Chem Soc* 62:815-818.

Kittelson, D. B., Watts, W. F., Johnson, J. P., Rowntree, C., Payne, M., Goodier, S., Warrens, C., Preston, H., Zink, U., Ortiz, M., Goersmann, C., Twigg, M. V., Walker, A. P. and Caldow, R. (2006). On-road evaluation of two Diesel exhaust aftertreatment devices. *J Aerosol Sci* 37:1140-1151.

Kleeman, MJ, Hughes, LS, Allen, JO and GR Cass (1999). Source contributions to the size and composition distribution of atmospheric particles: Southern California in September 1996. *Environmental Science and Technology*, **33**, 4331 – 4341.

Kleinman, MT, Hamade, A, Meacher, D, Oldham, M, Sioutas, C, Chakrabarti, L, Stram, D, Froines, JF and AK Cho (2005). Inhalation of concentrated ambient particulate matter near a heavily trafficked road stimulates angtigen-induced airway responses in mice. *Journal of the Air and Waste Management Association*, **55(9)**, 1277 – 1288.

Knothe, G. (2006). Analysis of oxidized biodiesel by H-1-NMR and effect of contact area with air. *Eur J Lipid Sci Tech* 108:493-500.

Landreman, A. P., Shafer, M. M., Hemming, J. C., Hannigan, M. P. and Schauer, J. J. (2008). A macrophage-based method for the assessment of the reactive oxygen species (ROS) activity of atmospheric particulate matter (PM) and application to routine (daily-24 h) aerosol monitoring studies. *Aerosol Sci Tech* 42:946-957.

Li, N, Sioutas, C, Froines, JR, Cho, A, Misra, C and A Nel (2003). Ultrafine particulate pollutants induce oxidative stress and mitochondrial damage. *Environmental Health Perspectives*, **111(4)**, 455 – 460.

Li, N, Kim, S, Wang, M, Froines, JR, Sioutas, C and A Nel (2002). Use of a stratified oxidative stress model to study the biological effects of ambient concentrated and diesel exhaust particulate matter. *Inhalation Toxicology*, **14(5)**, 459 – 486.

Lloyd, A. C. and Cackette, T. A. (2001). Diesel engines: Environmental impact and control. *J Air Waste Manage* 51:809-847.

Lough, GC, Schauer, JJ, Park, JS, Shafer, MM, DeMinter, JT and JP Weinstein (2005). Emissions of metals associated with motor vehicle roadways. *Environmental Science and Technology*, **39**, 826 – 836.

McDonald, J. D., Reed, M. D., Campen, M. J., Barrett, E. G., Seagrave, J. and Mauderly, J. L. (2007). Health effects of inhaled gasoline engine emissions. *Inhalation Toxicology* 19:107-116.

Miguel, A. H., Kirchstetter, T. W., Harley, R. A. and Hering, S. V. (1998). On-road emissions of particulate polycyclic aromatic hydrocarbons and black carbon from gasoline and diesel vehicles. *Environ Sci Technol* 32:450-455.

Mills, NL, Tonrqvist, H, Robinson, SD, Darnley, K, Gonzales, M, Boon, NA, MacNee, W, Donaldson, K, Blomber, A, Sandstrom, T and DE Newby (2005). Diesel exhaust inhalation causes vascular dysfunction and impaired endogenous fibrinolysis: an explanation for the increased cardiovascular mortality associated with air pollution. *J Am Coll Cardiol*, **45(3)**, 390a – 390a.

Nel, A (2005). Air pollution-related illness: effects of particles. *Science*, **308**, 804 – 806.

Ntziachristos, L, Samaras, Z., Rexeis, M and S Hausberger (2006). Diesel particle exhaust emissions from light duty vehicles and heavy duty engines. *J. Fuels Lubricants,* **115(4)**, 294–308.

Ntziachristos, L, Cho, AK, Froines, JR and C Sioutas (2007). Relationship between redox activity and chemical species of size fractionated particulate matter. *Part. Fibre Toxicol*, **4(5)**, doi:10.1186/1743-8977.

Pekkanen, J, Timonen, KL, Ruuskanen, J, Reponen, A and A Mirme (1997). Effects of ultrafine and fine particles in urban air on peak expiratory flow among children with asthmatic symptoms. *Environmental Research*, **74(1)**, 24 – 33.

Rogge, W. F., Hildemann, L. M., Mazurek, M. A., Cass, G. R. and Simoneit, B. R. T. (1993). Sources of Fine Organic Aerosol .2. Noncatalyst and Catalyst-Equipped Automobiles and Heavy-Duty Diesel Trucks. *Environ Sci Technol* 27:636-651.

Sakurai, H, Park, K, McMurry, PH, Zarling, DD, Kittelson, DB and PJ Ziemann (2003). Size-dependent mixing characteristics of volatile and nonvolatile components in diesel exhaust aerosols. *Environmental Science and Technology*, **37(24)**, 5487-5495

Schoonen, M. A. A., Cohn, C. A., Roemer, E., Laffers, R., Simon, S. R. and O'Riordan, T. (2006). Mineral-induced formation of reactive oxygen species. *Reviews in mineralogy and geochemistry* 64:179-221.

Schafer, M, Schafer, C, Ewald, N, Piper, HM and T Noll (2003). Role of redox signaling in the autonomous proliferative response of endothelial cells to hypoxia. *Circulation Research,* **92(9)**, 1010–1015.

Schauer, JJ, Kleeman, MJ, Cass GR and BRT Simoneit (2002). Measurement of emissions from air pollution sources. 5. C1 – C32 organic compounds from gasoline-powered motor vehicles. *Environmental Science and Technology*, **36**, 1169 – 1180.

Schauer, JJ, Kleeman MJ, Cass, GR and BRT Simoneit (2001). Measurements of emissions from air pollution sources. 3. C1-C29 organic compounds from fireplace combustion of wood. *Environmental Science and Technology*, **35**, 1716 – 1728.

Schauer, JJ, Kleeman, MJ, Cass, GR and BRT Simoneit (1999). Measurement of emissions from air pollution sources. 2. C1 – C29 organic compounds from medium duty diesel trucks. *Environmental Science and Technology*, **33**, 1578 – 1587.

Seagrave, J., McDonald, J. D., Bedrick, E., Edgerton, E. S., Gigliotti, A. P., Jansen, J. J., Ke, L., Naeher, L. P., Seilkop, S. K., Zheng, M. and Mauderly, J. L. (2006). Lung toxicity of ambient particulate matter from southeastern US sites with different contributing sources: Relationships between composition and effects. *Environmental Health Perspectives* 114:1387-1393.

Sheesley, RJ (2004). Composition and aquatic toxicity of organic aerosols. Ph.D. Dissertation, University of Wisconsin-Madison. Department of Civil and Environmental Engineering.

Shi, X. Y., Pang, X. B., Mu, Y. J., He, H., Shuai, S. J., Wang, J. X., Chen, H. and Li, R. L. (2006). Emission reduction potential of using ethanol-biodiesel-diesel fuel blend on a heavy-duty diesel engine. *Atmospheric Environment* 40:2567-2574.

Stayner, L, Dankovic, D, Smith, R and K Steenland (1998). Predicted lung cancer risk among miners exposed to diesel exhaust particles. *Am J Ind Med*, **34(3)**, 207 – 219.

Stone, E. A., Snyder, D. C., Sheesley, R. J., Sullivan, A. P., Weber, R. J. and Schauer, J. J. (2008). Source apportionment of fine organic aerosol in Mexico City during the MILAGRO experiment 2006. *Atmos Chem Phys* 8:1249-1259.

Tsai, F. C., Apte, M. G. and Daisey, J. M. (2000). An exploratory analysis of the relationship between mortality and the chemical composition of airborne particulate matter. *Inhal Toxicol* 12:121-135.

Turpin, BJ and HJ Lim (2001). Species contributions to PM2.5 mass concentrations: revisiting common assumptions for estimating organic mass. *Aerosol Science and Technology*, **35(1)**, 602 – 610.

Vaaraslahti, K., Virtanen, A., Ristimaki, J. and Keskinen, J. (2004). Nucleation mode formation in heavy-duty diesel exhaust with and without a particulate filter. *Environ Sci Technol* 38:4884-4890.

Valavanidis, A., Salika, A. and Theodoropoulou, A. (2000). Generation of hydroxyl radicals by urban suspended particulate air matter. The role of iron ions. *Atmospheric Environment* 34:2379-2386.

Verma, V., Polidori, A., Schauer, J. J., Shafer, M. M., Cassee, F. R. and Sioutas, C. (2009). Physicochemical and Toxicological Profiles of Particulate Matter in Los Angeles during the October 2007 Southern California Wildfires. *Environ Sci Technol* 43:954-960.

Vogl, G and EF Elstner (1989). Diesel soot particles catalyze the production of oxy-radicals. *Toxicology Letters*, **47(1)**, 17 – 23.

Wang, W. G., Lyons, D. W., Clark, N. N., Gautam, M. and Norton, P. M. (2000). Emissions from nine heavy trucks fueled by diesel and biodiesel blend without engine modification. *Environ Sci Technol* 34:933-939.

Wang, Y. F., Huang, K. L., Li, C. T., Mi, H. H., Luo, J. H. and Tsai, P. J. (2003). Emissions of fuel metals content from a diesel vehicle engine. *Atmospheric Environment* 37:4637-4643.

Westerdahl, D, Fruin, S, Sax, T, Fine, PM and C Sioutas (2005). Mobile platform measurements of ultrafine particles and associated pollutant concentrations on freeways and residential streets in Los Angeles. *Atmospheric Environment*, **39(20)**, 3597 – 3610.

Xia, T, Korge, P, Weiss, JN, Li, N, Venkatesen, MI and C Sioutas (2004). Quinones and aromatic chemical compounds in particulate matter induce mitochondrial dysfunction: implications for ultrafine particle toxicity. *Environmental Health Perspectives*, **112(14)**, 1347 – 1358.

Zhang, YX, Schauer, JJ, Shafer, MM, Hannigan MP and SJ Dutton (2008). Source apportionment of in vitro reactive oxygen species bioassay activity from atmospheric particulate matter. *Environmental Science and Technology*, **42(19)**, 7502 – 7509.

Zhao, Y, Bein, KJ, Wexler, AS, Misra, C, Fine, PM and C Sioutas (2005). Field evaluation of the versatile aerosol concentration enrichment system (VACES) particle concentrator coupled to the rapid single-particle mass spectrometer (RSMS-3). *Journal of Geophysical Research – Atmospheres*, **110**, D07S02, doi:10.1029/2004JD004644, (D7).

Zielinska, B., Sagebiel, J., Arnott, W. P., Rogers, C. F., Kelly, K. E., Wagner, D. A., Lighty, J. S., Sarofim, A. F. and Palmer, G. (2004). Phase and size distribution of polycyclic aromatic hydrocarbons in diesel and gasoline vehicle emissions. *Environ Sci Technol* 38:2557-2567.

Table 1: General Information about the make, model, emission standard, engine capacity, emission control, mileage and fuel used in each vehicle configuration.

Make	Model	Emission standard	Engine Capacity [l]	Emission Control	Fuel	Mileage (×10³ km)
Honda	Accord i-CTDi	Euro 4	2.2	Closed-coupled oxidation catalyst (pre-cat) + exhaust gas recirculation (EGR) + main underbody oxidation catalyst	Diesel 10 ppm S	45
Honda	Accord i-CTDi	Euro 4+	2.2	Pre-cat + EGR+ Ceramic catalyzed DPF	Diesel 10 ppm S	
Toyota	Corolla	Euro 3	1.8	Three-way catalytic converter	Unleaded Gasoline RON95	100
VW	Golf TDi	Euro 2	1.9	Oxidation catalyst	Neat soybean biodiesel	168
VW	Golf TDi	Euro 1	1.9	-	Diesel 50 ppm S	

Table 2: Fuel properties of the (a) petrodiesel and (b) biodiesel used in the Golf vehicle

a)

Properties	Units	Petroleum Diesel	EN 590 Limits	Test Method
Viscosity (40°C)	$mm^2\,s^{-1}$	3.61	2.00-4.50	EN ISO 3104
Density (15°C)	$g\,cm^{-3}$	0.8345	0.820-0.845	EN ISO 3675
Flash Point	°C	71	55 min	EN 22719
Sulfur Content	$\mu g\,g^{-1}$	29	50 max	EN ISO 20846
Water Content	$\mu g\,g^{-1}$	52	200 max	EN ISO 12937
Cold Filter Plugging Point (CFPP)	°C	-9	+ 5 max	EN 116
Cetane number		55.5	51 min	EN ISO 5165
Distillation				EN ISO 3405
Initial Boiling Point (IBP)		179		
10%		220		
50%		281		
90%		344		
Final Boiling Point (FBP)		367		
Gross Heating Value	$cal\,g^{-1}$	10900	-	IP 12

b)

Property	Units	Biodiesel	EN 14214 Limits	Test Method
Viscosity, 40 °C	mm^2 s^{-1}	4.4	3.5-5.0	EN ISO 3104
Density, 15°C	g cm^{-3}	0.8816	0.860-0.900	EN ISO 12185
Flash point	°C	>166	120 min	EN ISO 3679
Sulfur content	µg g^{-1}	2.0	10.0 max	EN ISO 20846
Water content	µg g^{-1}	450	500 max	EN ISO 12937
Copper strip corrosion (3h at 50 °C)	Rating	1A	Class 1	EN ISO 2160
CFPP	°C	-7	-5 max	EN 116
Cetane number		52	51 min	EN ISO 5165
Sulfated ash content	%(m/m)	<0.01	0.02 max	ISO 3987
Oxidation stability, 110 °C	Hours	4.6	6 min	EN 14112
Iodine number		122	120 max	EN 14111
Acid value	mg KOH g^{-1}	0.4	0.50 max	EN 14104
Monoglyceride content	%(m/m)	0.77	0.80 max	EN 14105
Diglyceride content	%(m/m)	0.19	0.20 max	EN 14105
Triglyceride content	%(m/m)	0.11	0.20 max	EN 14105
Free glycerol	%(m/m)	0.05	0.02 max	EN 14106
Total glycerol	%(m/m)	0.23	0.25 max	EN 14105
Methanol content	%(m/m)	0.12	0.20 max	EN 14110
Ester content	%(m/m)	96.6	96.5 min	
Linolenic acid methyl ester	%(m/m)	5.77	12 max	
Group I Metals (Na+K)	µg g^{-1}	<0.01, 0.9	5.0 max	EN 14108 EN 14109
Phosphorous content	µg g^{-1}	5	10 max	EN 14107
Gross heating value	cal g^{-1}	9228	-	IP 12

Table 3: Mass and chemical species emissions (mg/kg) for each vehicle/configuration

	PM mass (mg/km)	OC (mg/km)	EC (mg/km)	WSOC (mg/km)	nitrate (mg/km)	sulfate (mg/km)	ammonium (mg/km)	sum of inorganic ions (mg/km)
Accord diesel	27.1	4.92	19.6	0.91	0.38	0.07	0.02	1.00
DPF-Accord diesel	0.63	0.51	0.03	0.10	0.08	0.10	0.02	0.31
Corolla gasoline	2.41	0.95	0.05	0.34	0.01	0.99	0.29	1.46
Golf diesel	72.1	24.2	39.1	1.48	0.14	0.14	0.02	0.64
Golf biodiesel	41.2	24.4	6.73	1.42	1.18	0.26	0.01	2.79

Table 4: Emission factors (µg/km) of PAHs, hopanes, steranes, alkanes and organic acid (OA)

	Accord Diesel	DPF-Accord	Corolla Gasoline	Golf Diesel	Golf Biodiesel
∑PAHs	2.55±0.43	BDL	0.67±0.08	16.5±1.4	10.4±0.9
∑PAHs, MW ≤ 228	2.55±0.43	BDL	0.20±0.05	15.6±1.4	7.76±0.90
∑PAHs, MW = 252	BDL	BDL	0.22±0.04	0.90±0.16	1.34±0.19
∑PAHs, MW ≥ 276	BDL	BDL	0.25±0.04	BDL	1.34±0.2
∑Hopanes	0.94±0.15	0.01±0.02	0.09±0.03	67.9±5.5	59.5±4.8
∑Steranes	BDL	BDL	BDL	23±1.9	20.2±1.6
∑Alkanes	197±30	6.95±5.34	9.78±3.09	981±84	125±27
∑Organics Acids	1.04±3.74	6.67±4.84	7.13±4.95	342±43	5240±355
∑OA, C9-14	BDL	1.32±1.12	1.71±1.33	11.3±5.0	17.7±6.3
∑OA, C15-29	1.04±3.74	5.35±4.70	5.42±4.77	331±43	5220±354

Table 5 Emission factors of selected trace elements and metals (ng/km)

	Accord Diesel	DPF-Accord	Corolla Gasoline	Golf Diesel	Golf Biodiesel
Al	148±43	20.6±12.3	21.1±12.8	1160±38	83.1±27.2
Ca	15100±1340	BDL	29700±742	118000±2080	54200±1740
Fe	5.23±20.5	10.0±8.6	622±10	618±17	428±19
Mg	5100±127	260±45	1590±69	4740±140	8200±176
Na	17700±566	BDL	4760±160	25300±356	149000±2650
P	4590±148	254±49	3670±56	31800±682	29900±604
S	24500±1460	30800±1170	301000±6350	81400±1660	78000±1130
K	10300±581	BDL	4050±298	13500±953	524000±28600
V	37.8±2.9	BDL	5.26±0.84	27.3±1.6	47.2±2.1
Cr	341±7	67.6±4.6	46.4±6.5	245±7	247±8
Mn	124±24	35.3±11.2	1640±16	426±23	432±23
Co	5.78±0.70	2.85±0.69	17.5±0.5	23.2±0.9	64.8±1.8
Ni	160±21	104±10	158±10	196±21	59.2±18.7
Cu	BDL	BDL	708±8	BDL	46.3±11.0
Zn	7020±164	372±65	2260±60	22300±187	22300±403
Cd	5.23±0.79	0.82±0.28	2.69±0.48	5.53±0.88	4.08±0.96
Ba	142±26	BDL	42.1±10.0	185±21	199±19
Pb	18.2±0.8	2.39±0.35	27.9±0.4	247±2	14.1±0.7

Table 6 Correlations coefficients, r, among selected PM chemical constituents

	Mg	Al	P	S	K	Ca	V	Cr	Mn	Fe	Co	Ni	Zn	Cd	Ba	Pb	Σ PAHs	Σ PAHs, MW ≤228	Σ PAHs, MW=252	Σ Hopanes	Σ Alkanes	Σ Organic Acids	Σ OA, C9-14	Σ OA, C15-29
Na	0.84	-0.10	0.68	-0.17	**0.99**	0.26	0.75	0.38	-0.12	0.21	**0.96**	-0.70	0.71	0.27	0.67	-0.13	0.46	0.35	0.85	0.64	-0.05	**0.99**	0.87	**0.99**
Mg		0.21	0.76	-0.29	0.77	0.46	**0.98**	0.79	-0.22	0.20	0.79	-0.28	0.84	0.73	**0.94**	0.15	0.64	0.57	0.77	0.70	0.28	0.77	0.77	0.77
Al			0.66	-0.16	-0.21	**0.90**	0.19	0.35	-0.14	0.47	0.02	0.64	0.63	0.61	0.52	**0.99**	0.84	**0.90**	0.39	0.69	**1.00**	-0.17	0.36	-0.17
P				-0.16	0.59	0.88	0.65	0.46	-0.11	0.58	0.76	-0.05	**0.99**	0.62	0.86	0.64	**0.96**	0.92	**0.94**	0.99	0.69	0.62	**0.93**	0.62
S					-0.13	0.04	-0.40	-0.59	**1.00**	0.69	0.06	0.22	-0.24	-0.18	-0.30	-0.04	-0.21	-0.23	-0.04	-0.19	-0.21	-0.13	-0.13	-0.13
K						0.15	0.66	0.27	-0.09	0.17	**0.95**	-0.78	0.61	0.14	0.56	-0.24	0.35	0.23	0.80	0.56	-0.17	**1.00**	0.82	**1.00**
Ca							0.37	0.33	0.07	0.72	0.41	0.41	0.84	0.66	0.70	**0.92**	**0.95**	**0.96**	0.71	**0.88**	**0.91**	0.19	0.66	0.19
V								**0.89**	-0.33	0.04	0.65	-0.21	0.76	0.78	**0.93**	0.11	0.56	0.51	0.64	0.59	0.27	0.66	0.63	0.66
Cr									-0.52	-0.19	0.24	0.12	0.59	0.86	0.83	0.25	0.50	0.50	0.31	0.41	0.43	0.27	0.32	0.27
Mn										0.72	0.11	0.23	-0.19	-0.11	-0.22	-0.02	-0.17	-0.19	0.01	-0.15	-0.18	-0.09	-0.09	-0.09
Fe											0.47	0.28	0.49	0.29	0.32	0.56	0.55	0.53	0.59	0.56	0.44	0.20	0.50	0.20
Co												-0.58	0.76	0.28	0.66	0.02	0.55	0.44	**0.93**	0.72	0.05	**0.96**	**0.92**	**0.96**
Ni													-0.06	0.45	0.03	0.67	0.19	0.30	-0.33	-0.05	0.62	-0.76	-0.40	-0.76
Zn														0.70	**0.92**	0.59	**0.95**	**0.91**	**0.92**	**0.97**	0.67	0.65	**0.91**	0.64
Cd															**0.88**	0.57	0.69	0.70	0.43	0.56	0.68	0.15	0.38	0.15
Ba																0.47	0.82	0.79	0.77	0.81	0.59	0.58	0.75	0.57
Pb																	0.82	0.88	0.38	0.67	**0.98**	-0.20	0.34	-0.20
Σ PAHs																		**0.99**	0.82	**0.97**	0.86	0.39	0.80	0.39
Σ PAHs, MW≤228																			0.74	**0.93**	**0.92**	0.28	0.72	0.28
Σ PAHs, MW=252																				**0.93**	0.41	0.82	**0.99**	0.82
Σ Hopanes																					0.71	0.60	**0.92**	0.59
Σ Alkanes																						-0.13	0.38	-0.13
Σ Organic Acids																							0.85	**1.00**
Σ OA, C9-14																								0.85
Σ OA, C15-29																								

Table 7: DTT consumption rates (expressed in nmol/(min-µg) and nmol/(min-km)) for each vehicle configuration

	DTT consumption rate	
	nmol/(min × µg) ± SD	nmol/(min × km) ± SD
Accord diesel	0.023 ± 0.002	624 ± 54.3
DPF-Accord diesel	0.019 ± 0.002	12.0 ± 1.3
Corolla gasoline	0.012 ± 0.001	29.1 ± 2.4
Golf diesel	0.018 ± 0.003	1300 ± 216
Golf biodiesel	0.025 ± 0.003	1040 ± 124

Table 8: ROS activity (µg of Zymosan units/km)

	Accord Diesel	DPF-Accord	Corolla Gasoline	Golf Diesel	Golf Biodiesel
ROS activity	BDL	BDL	20.1±1.5	17.7±2.7	10.2±2.4

Table 9: Pearson correlation coefficients (r), corresponding significance levels (P), regression slopes (m) (nmol/(min-km)) or (nmol/(min-µg)), and y-intercepts (nmol/(min-km)) between DTT consumption rates (nmol/(min-km)) and various chemical species ((mg/km) or (µg/km))

species	EC	WSOC	WISOC	OC	chloride	nitrate	phosphate	sulfate	sodium	ammonium
Pearson R	0.80	0.98	0.93	0.94	0.28	0.51	0.16	−0.45	0.69	−0.56
P-value	0.11	<0.01	0.02	0.02	0.72	0.38	0.84	0.44	0.20	0.33
regression slope	27.9	915	46.4	44.5	6.43	0.61	4.20	−0.68	1.72	−2.68
y-intercept	234	−177	128	1310	560	380	656	813	106	800

Table 10   Pearson correlation coefficients (R), corresponding significance levels (P), regression slopes (m) (µg of Zymosan units/ng) or [nmol/(min×ng)], and y-intercepts(µg of Zymosan units/km) or [nmol/(min×km)] between ROS activity (µg of Zymosan units/km), DTT consumption rates [nmol/(min×km)], and selected elemental species (ng/km)

		Al	Ca	Fe	K	Mg	Na	P	S	V	Cr	Mn	Co	Ni	Zn	Cd	Ba	Pb	ROS
ROS	R	0.43	0.66	0.99	0.04	0.07	0.08	0.46	0.77	-0.07	-0.27	0.79	0.35	0.37	0.36	0.24	0.21	0.53	
	P	0.47	0.23	<0.01	0.99	0.91	0.90	0.44	0.13	0.91	0.66	0.11	0.57	0.55	0.55	0.70	0.73	0.35	
	m	8.36	0.13	30.2	0.00	0.22	0.01	0.28	0.06	-34.2	-20.1	11.6	133	64.6	0.32	1150	22.6	48.6	
	b	7.20	3.74	-0.57	9.40	8.70	9.14	5.65	2.94	10.4	13.4	3.40	6.56	0.86	6.13	5.37	7.03	6.58	
DTT	R	0.72	0.83	0.36	0.44	0.82	0.56	0.92	-0.37	0.79	0.75	-0.31	0.57	0.12	0.96	0.83	0.95	0.67	0.24
	P	0.17	0.08	0.56	0.46	0.09	0.33	0.03	0.54	0.11	0.15	0.61	0.31	0.85	0.01	0.08	0.01	0.22	0.69
	m	859	10.5	670	1.11	152	5.24	34.8	-1.91	22631	3420	-282	13354	1299	52.2	248386	6285	3746	15.0
	b	355	146	375	479	-5.0	395	112	798	69.4	-46.3	751	296	425	34.9	-310	-113	369	457.5

Table 11 Pearson correlation coefficients (R), corresponding significance levels (P), regression slopes (m) [nmol/(min×µg)] or (µg of Zymosan units/µg), and y-intercepts [nmol/(min×km)] or (µg of Zymosan units/km) between DTT consumption rates [nmol/(min×km)], ROS activity (µg of Zymosan units/km), and selected organic species (µg/km)

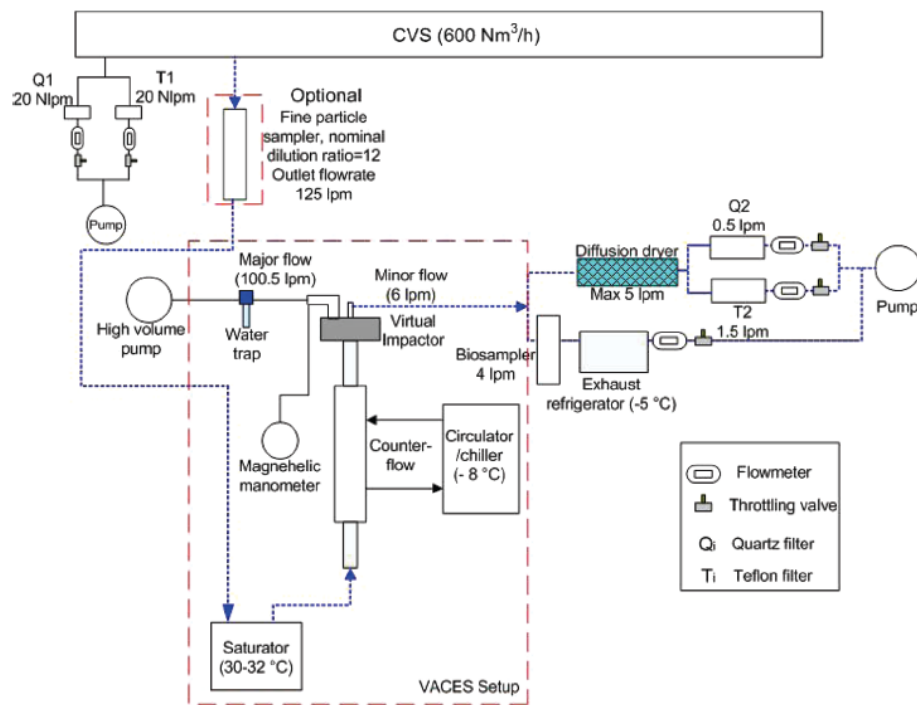|		∑PAHs	∑PAHs, MW ≤ 228	∑PAHS, MW = 252	∑Hopanes	∑Alkanes	∑Organic Acids	∑OA, C9-14	∑OA, C15-29	DTT
DTT	R	0.94	0.93	0.78	0.91	0.77	0.47	0.77	0.47	
	P	0.02	0.02	0.12	0.03	0.13	0.42	0.13	0.42	
	m	76.9	82.3	757	15.2	1.10	0.12	57.8	0.12	
	b	142	172	228	212	311	468	231	469	
ROS	R	0.45	0.43	0.46	0.44	0.40	0.07	0.37	0.07	0.24
	P	0.45	0.46	0.44	0.46	0.51	0.91	0.55	0.91	0.69
	m	0.60	0.63	7.22	0.12	0.01	0.00	0.45	0.00	0.00
	b	6.03	6.33	6.04	6.53	7.16	9.27	6.73	9.28	7.21

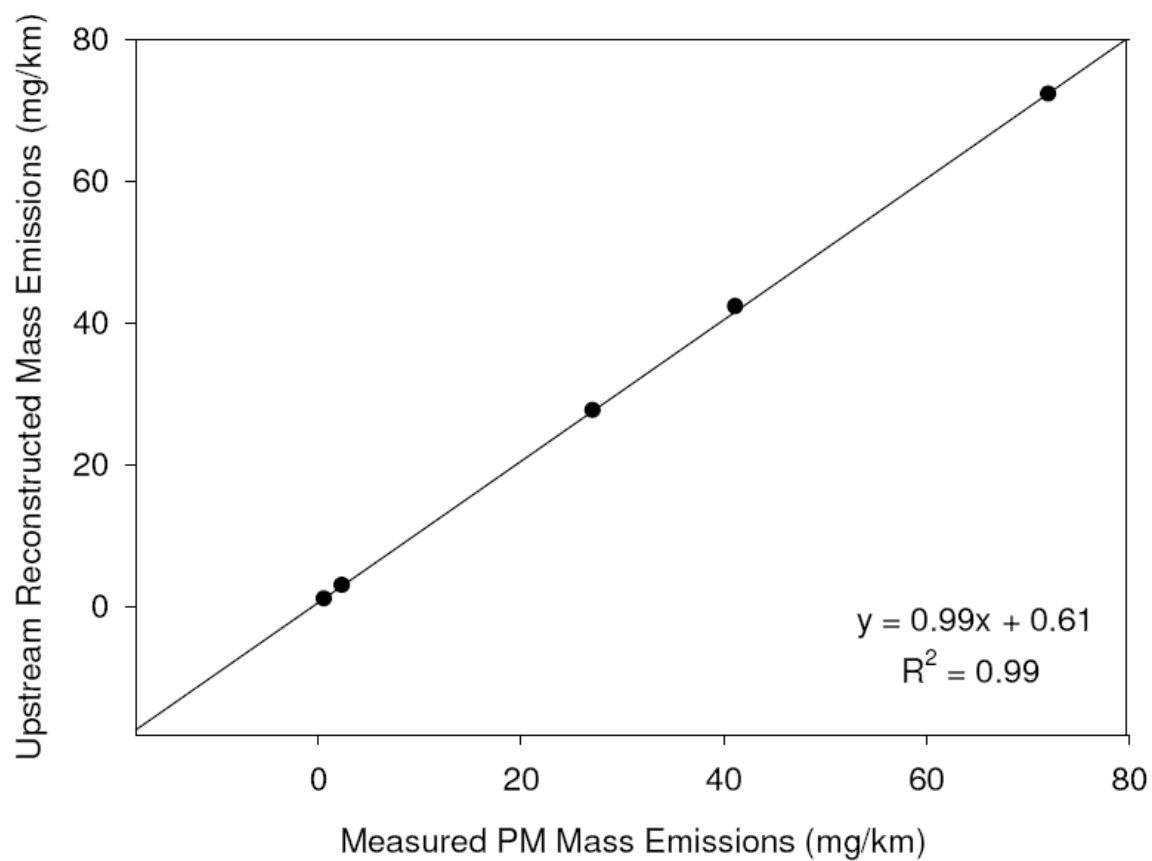**FIGURE 1.** Schematic of the sampling system used for particulate matter collection.

Figure 2: Correlation between reconstructed mass emissions (sum of EC, OM and ions) and gravimetrically-determined PM mass emissions (mg/km)
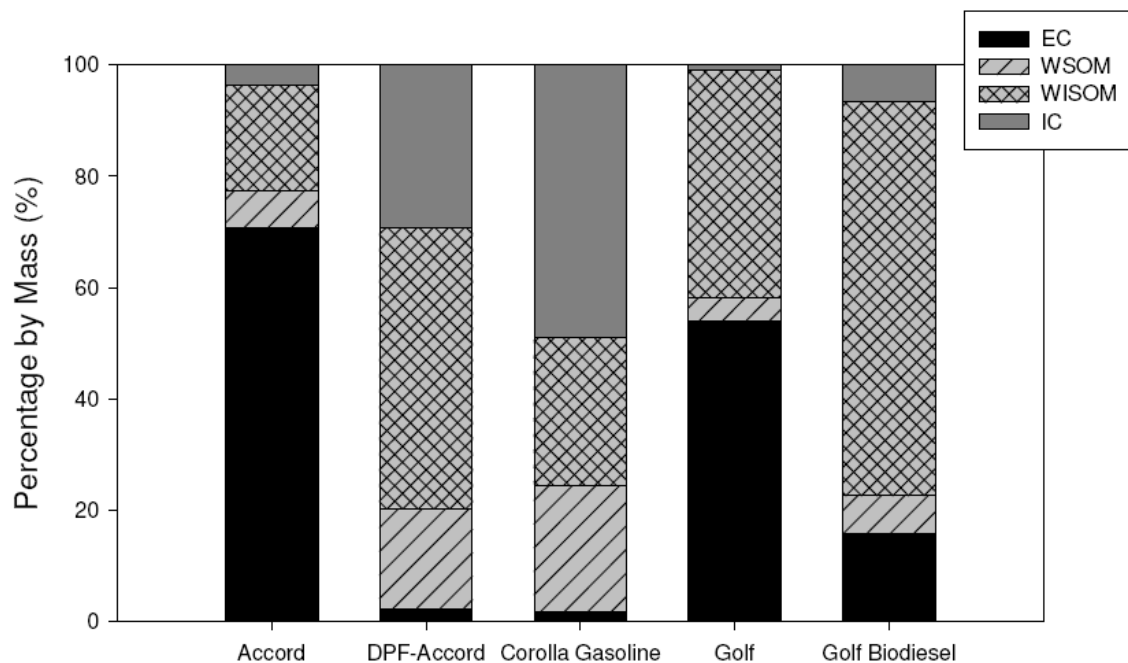
Figure 3: Percentage contributions of different chemical species (elemental carbon (EC), water soluble organic matter (WSOM), water insoluble organic matter (WISOM) and inorganic ions (IC) to the total emission rate from each of the tested vehicles.
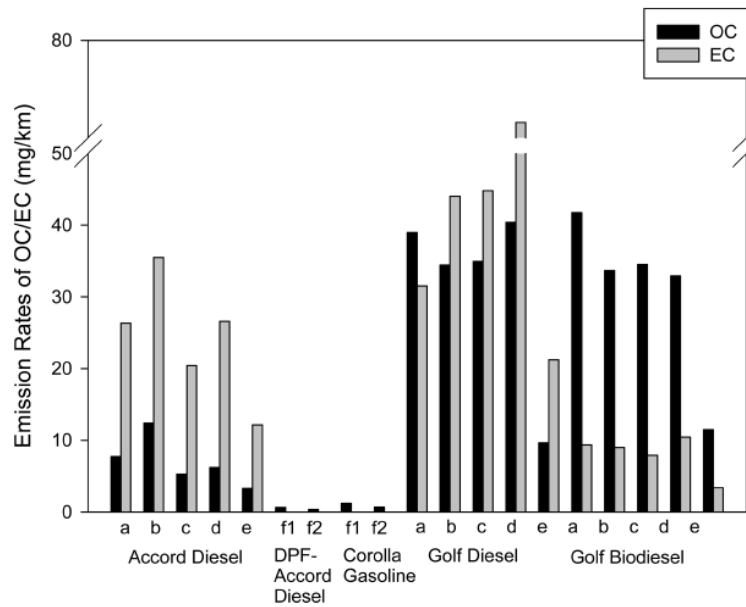
Figure 4: Emission rates (mg/km) of organic carbon (OC) and elemental carbon (EC) for each vehicle/configuration: (a) NEDC cycle, (b) ARTEMIS urban cycle, (c) ARTEMIS road cycle, (d) ARTEMIS motorway cycle, (e) 90 km/h steady state, (f1) all cycles composite on the first day, and (f2) all cycles composite on the second day.
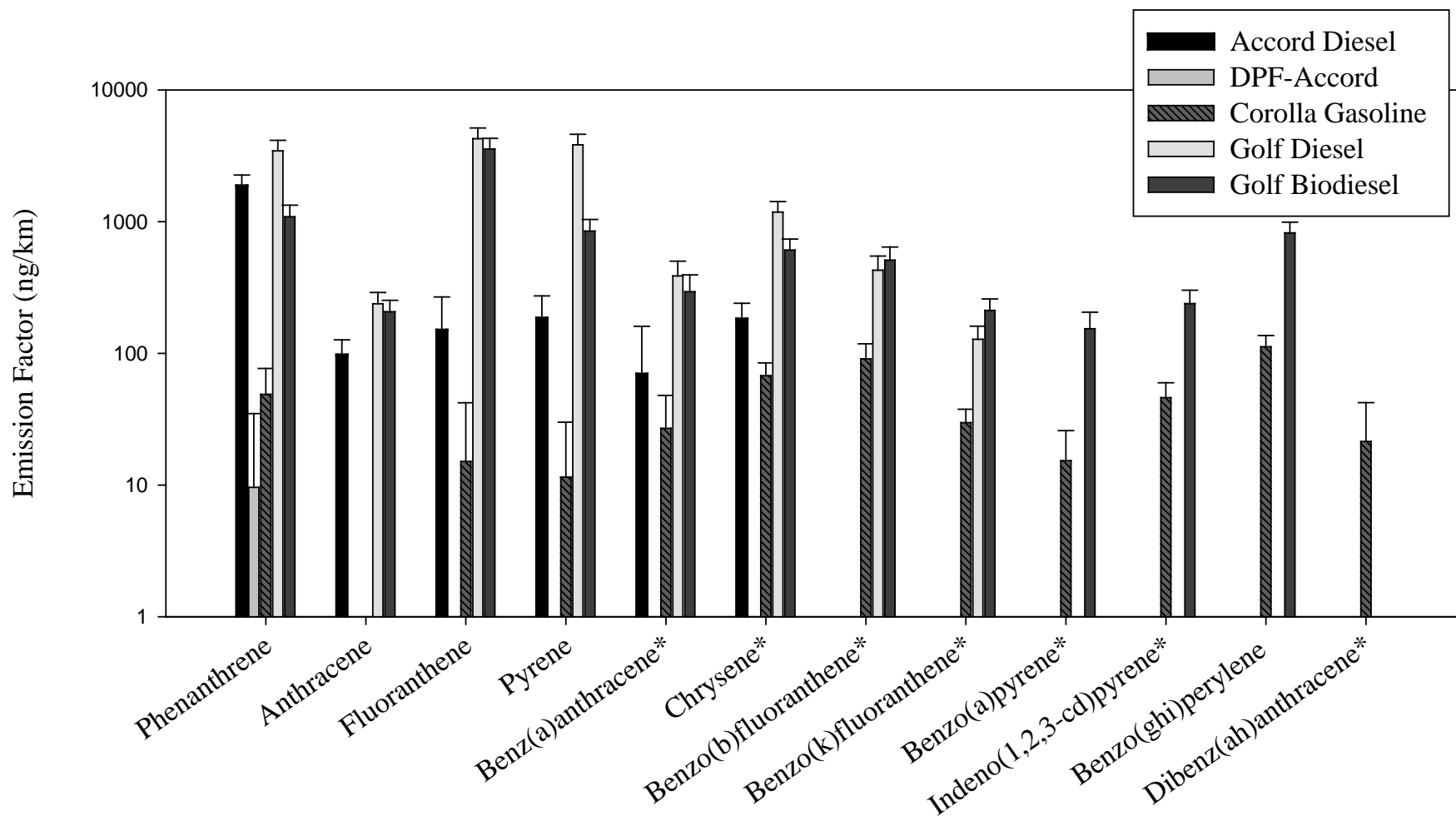
Figure 5 Emission factors (ng/km) of 12 priority polycyclic aromatic hydrocarbons (PAHs) classified by the U.S. EPA
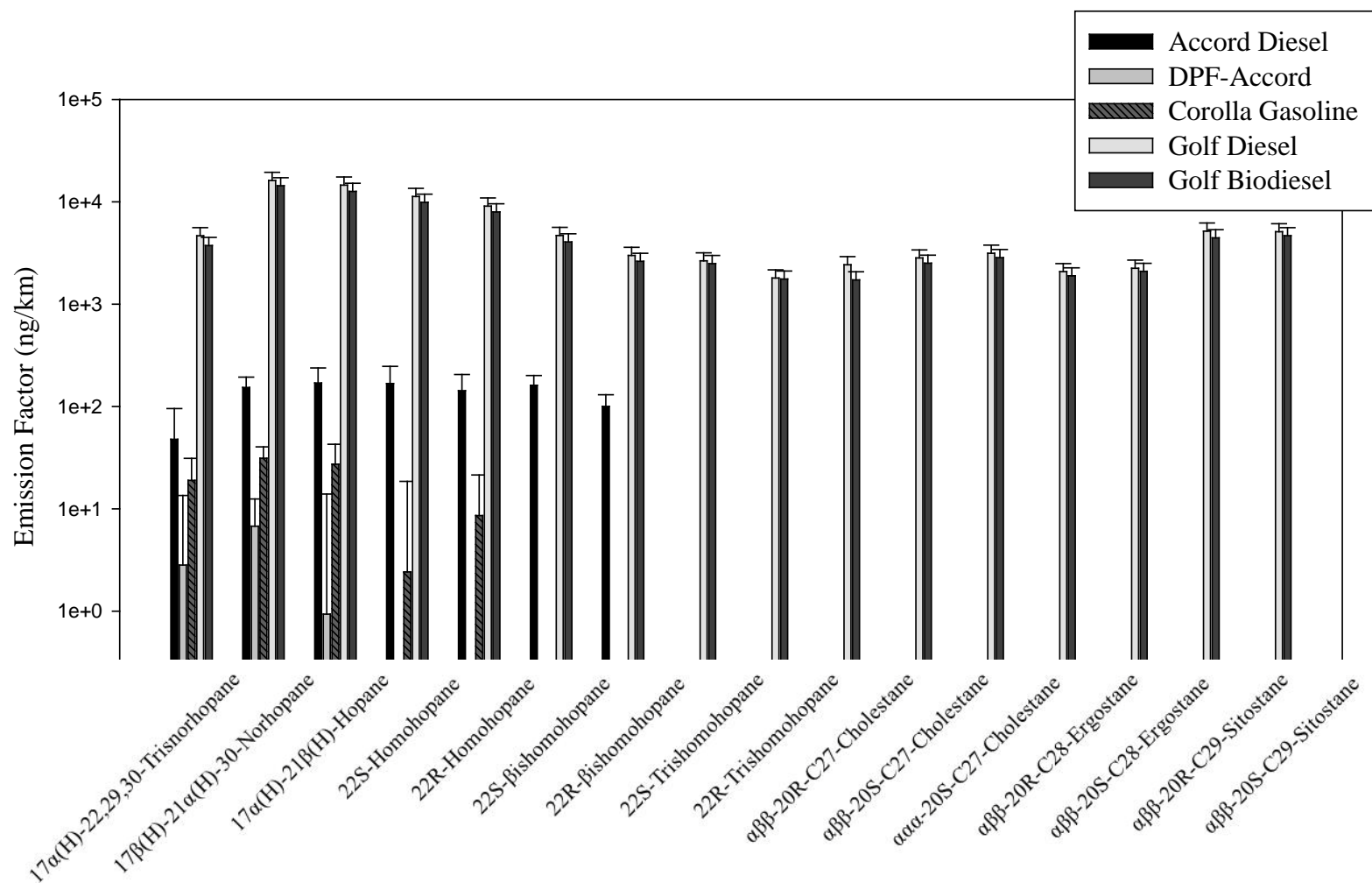
Figure 6 Emission factors (ng/km) of hopanes and steranes

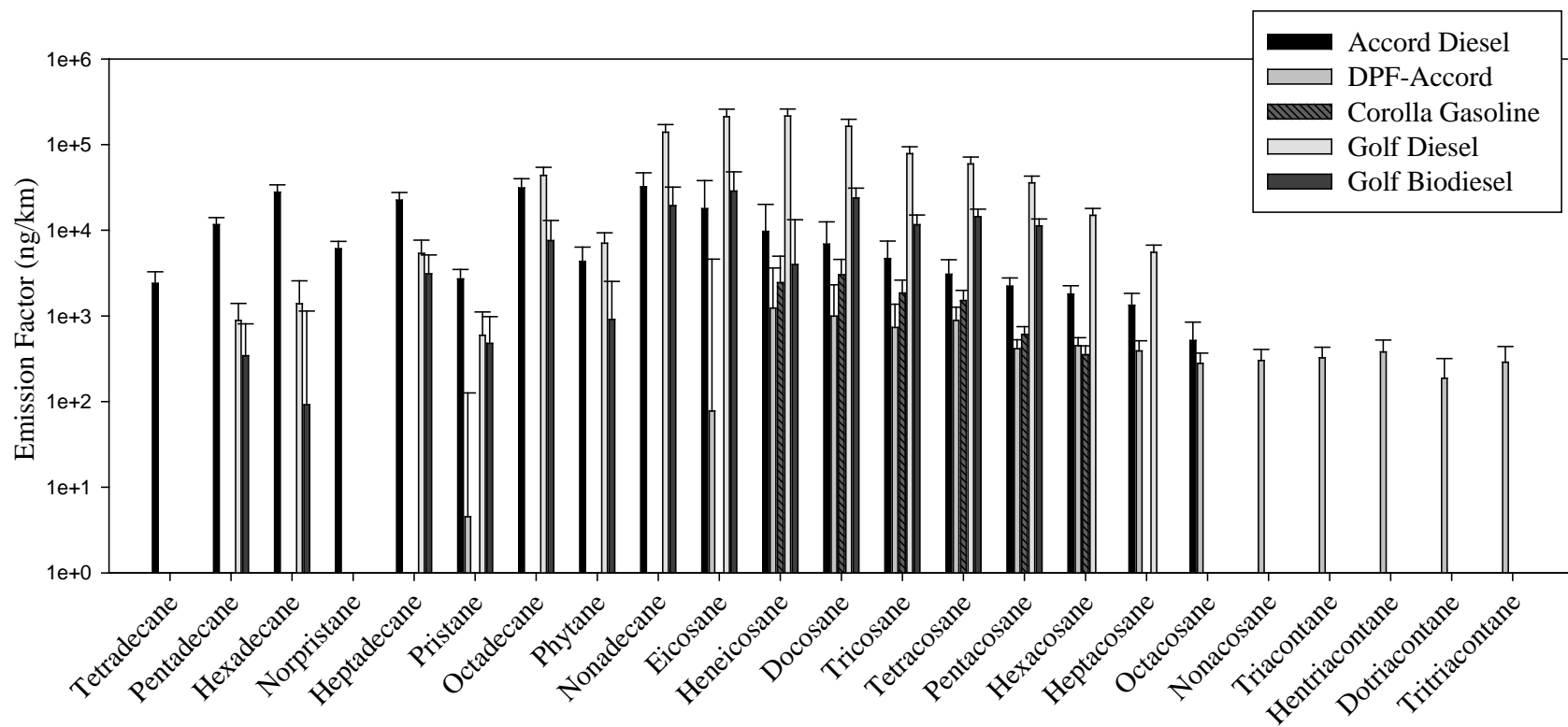**Figure 7** Emission factors (ng/km) of selected n-alkanes
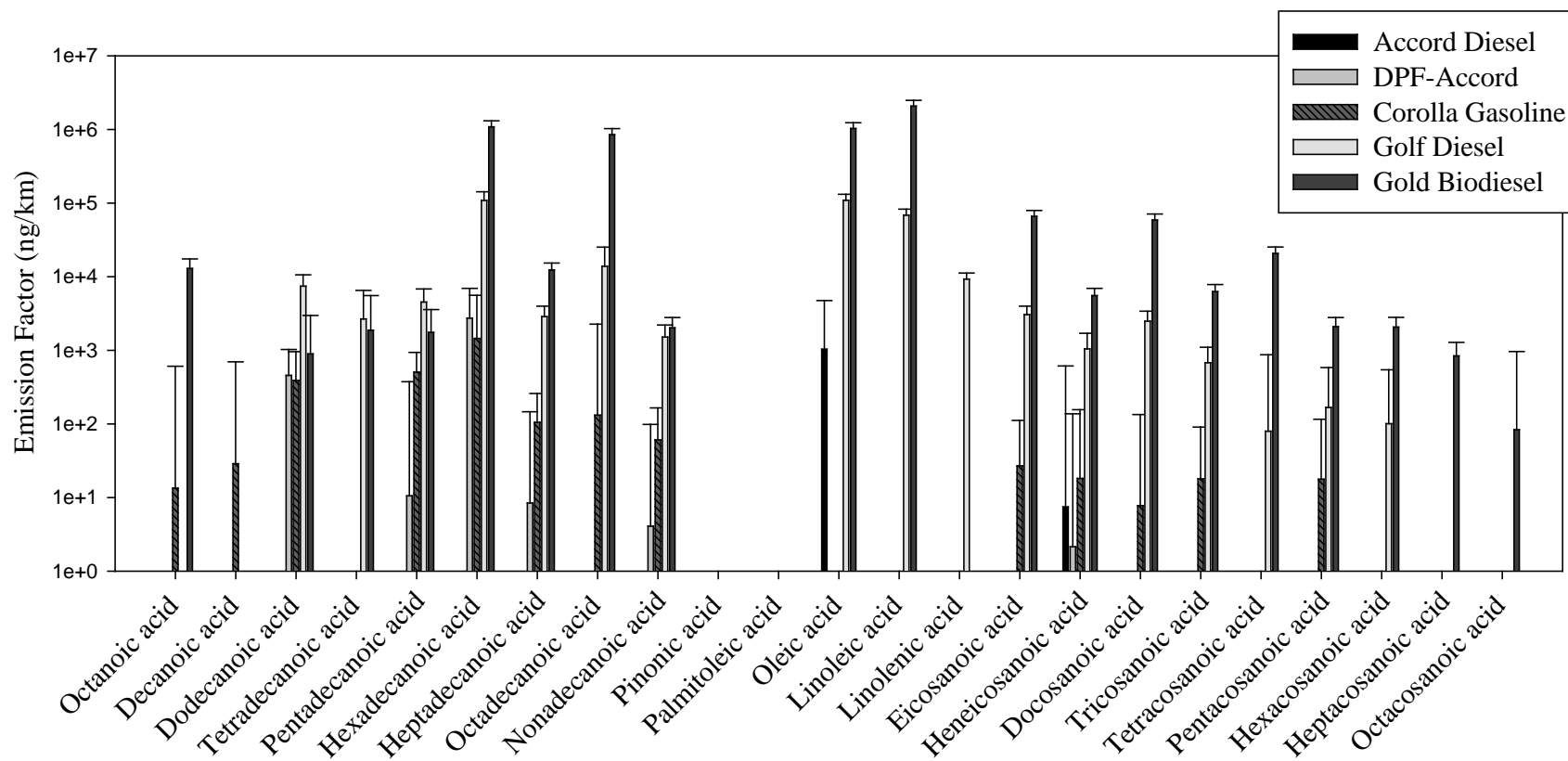
Figure 8 Emission factors (ng/km) of selected organic acids
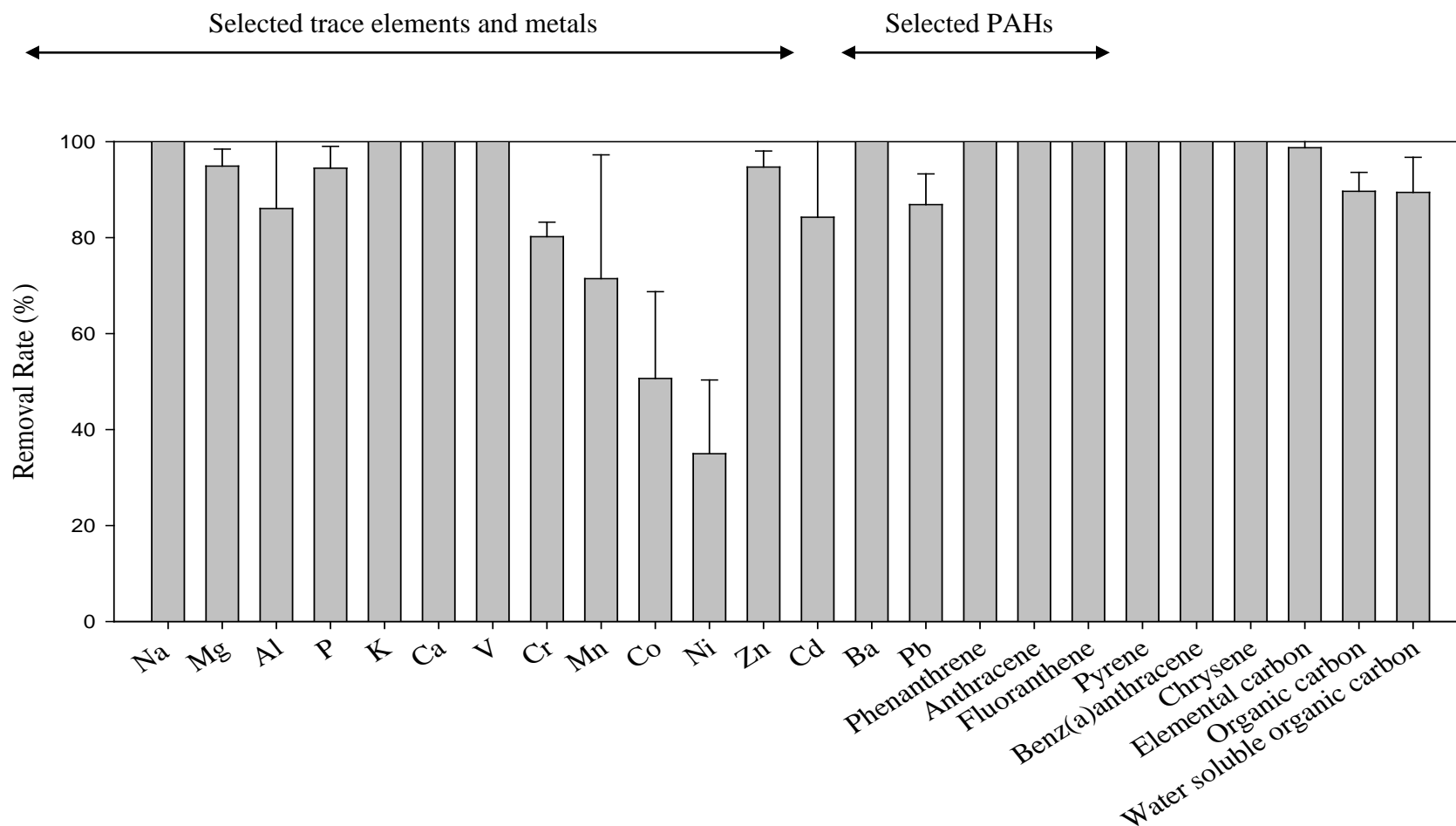
Figure 9 DPF removal rates (%) of selected trace elements and metals, selected PAHs, elemental carbon, organic carbon, and water soluble organic carbon of the Honda Accord vehicle
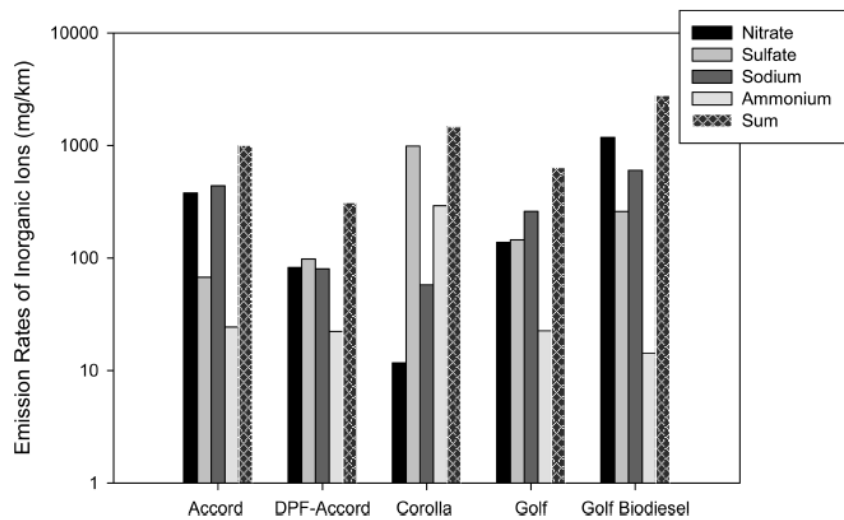
Figure 10: Emission rates of selected inorganic ions (mg/km) for each vehicle/configuration
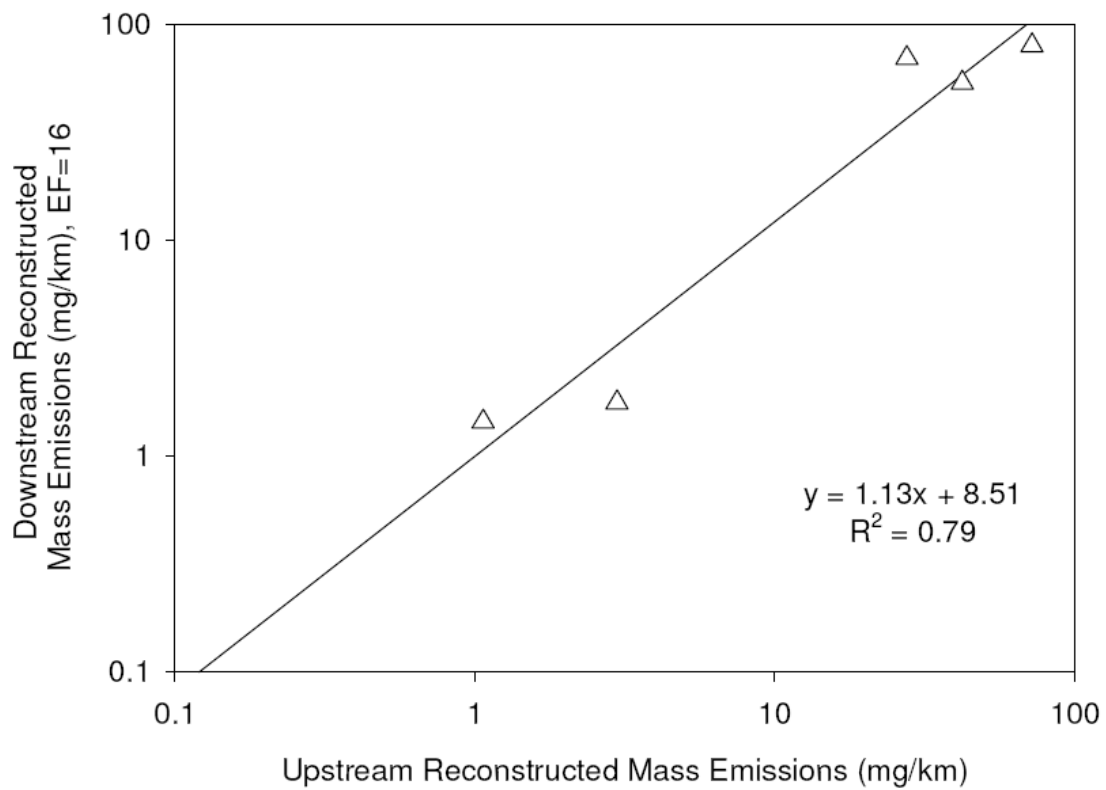
Figure 11: Comparison between the PM masses reconstructed as the sum of EC, OM and inorganic ion measurements from filters collected "upstream" and "downstream" of the VACES. A theoretical enrichment factor was used for the calculations (as discussed in the text).
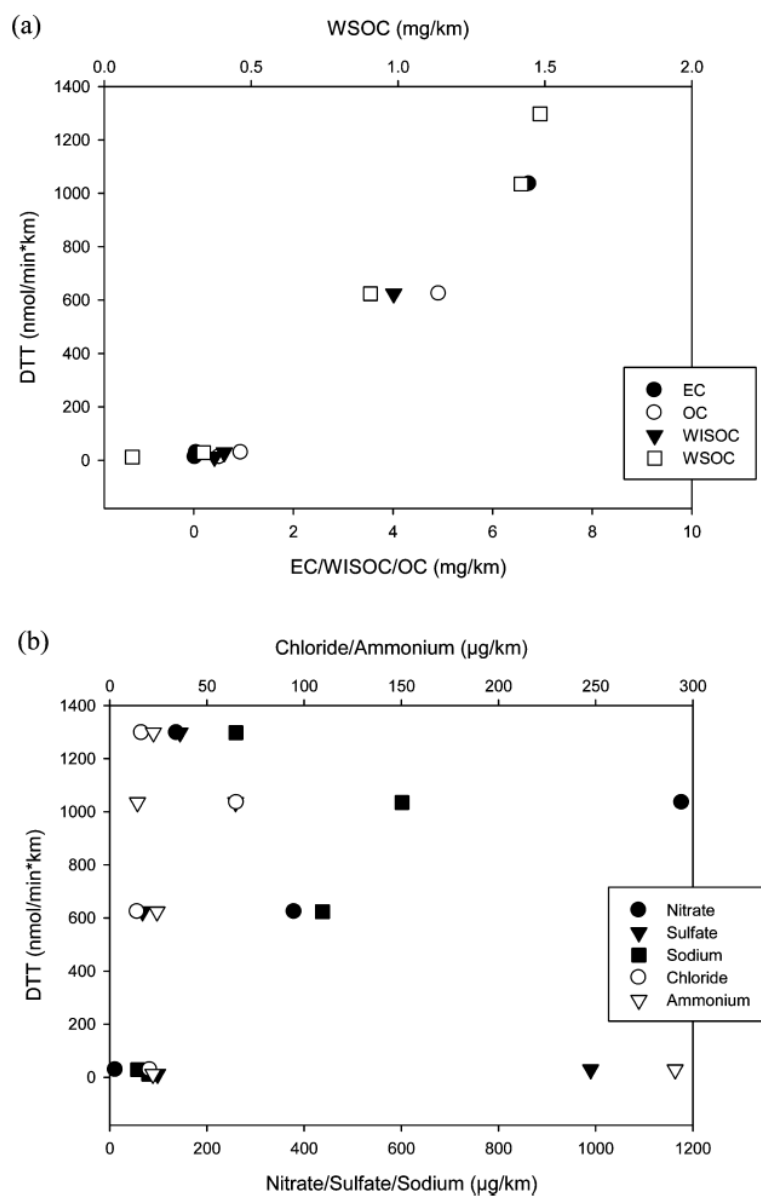
Figure 12: Correlation plots between chemical species and the corresponding DTT consumption rates of particulate matter from each vehicle configuration: (a) elemental carbon (EC), organic carbon (OC), water insoluble carbon (WISOC) and water soluble organic carbon (WSOC), (b) nitrate, sulfate, sodium, chloride and ammonium.

Appendix

Detection Limits

In the following table (shown by vehicle configuration):
a) Detection limit of selected trace elements and metals (ng/km)
b) Detection limit of selected PAHs (ng/km)
c) Detection limit of hopanes and steranes (ng/km)
d) Detection limit of selected n-alkanes (ng/km)
e) Detection limit of selected organic acids (ng/km)
f) Detection limit of ROS activity (µg of Zymosan units/km) and DTT consumption rate (nmol/(min-km))

	Accord Diesel	DPF-Accord	Corolla Gasoline	Golf Diesel	Golf Biodiesel
Na	219	115	131	147	1120
Mg	49.2	37.8	56.4	57.9	74.2
Al	16.5	10.3	10.5	15.7	11.4
P	56.9	40.8	45.6	282	254
S	565	981	5210	687	478
K	224	307	244	394	12100
Ca	517	458	609	859	731
Ti	2.65	2.96	2.89	2.65	2.22
V	1.11	0.736	0.69	0.647	0.864
Cr	2.8	3.83	5.3	2.96	3.34
Mn	9.4	9.37	13.3	9.42	9.81
Fe	7.9	7.18	8.36	7.1	7.93
Co	0.269	0.579	0.411	0.356	0.776
Ni	8.21	8.17	8.18	8.45	7.87
Cu	4.53	4.58	6.36	7.67	4.63
Zn	63.1	54	49.1	77.4	170
Cd	0.305	0.236	0.396	0.365	0.406
Ba	9.94	7.95	8.2	8.72	7.93
Pb	0.324	0.295	0.341	0.804	0.314
Phenanthrene	152	21.1	22.9	290	103
Anthracene	11.4	4.17	4.17	21.5	19.5
Fluoranthene	45.6	21.3	22.2	360	308
Acephenanthrylene	34.6	16.7	16.7	83.1	34.6
Pyrene	33.9	14.5	15.2	321	80.3
Benzo(ghi)fluoranthene	8.65	4.17	6.16	107	97.4
Cyclopenta(cd)pyrene	34.6	16.7	16.7	34.6	34.6
Benz(a)anthracene	35	16.7	17.2	47.2	42.6
Chrysene	22.3	8.33	13.9	99.2	54.2
1-Methylchrysene	8.65	4.17	4.17	8.65	8.65
Retene	26	12.5	16.2	26	26
Benzo(b)fluoranthene	34.6	16.7	22.4	49.5	55.2
Benzo(k)fluoranthene	8.65	4.17	6.42	13.7	19.8
Benzo(j)fluoranthene	8.65	4.17	4.17	8.65	8.65
Benzo(e)pyrene	26	12.5	18.4	38.7	46.8
Benzo(a)pyrene	17.3	8.33	8.7	17.3	21.6
Perylene	17.3	8.33	8.33	17.3	17.3
Indeno(1,2,3-cd)pyrene	17.3	8.33	11.2	17.3	26.5
Benzo(GHI)perylene	17.3	8.33	20.2	17.3	71.4
Dibenz(ah)anthracene	34.6	16.7	17	34.6	34.6
Picene	26	12.5	12.5	26	26
Coronene	26	12.5	17.3	26	35.2
17α(H)-22,29,30-Trisnorhopane	18.3	8.92	9.99	387	317
17β(H)-21α(H)-30-Norhopane	15.6	4.8	7.49	1340	1210
17α(H)-21β(H)-Hopane	26.5	10.9	12.7	1210	1070
22S-Homohopane	30.6	12.8	13.3	936	838
22R-Homohopane	24	9.82	10.5	754	674
22S-βishomohopane	15.2	4.17	4.17	387	342
22R-βishomohopane	11.6	4.17	4.17	248	221
22S-Trishomohopane	8.65	4.17	4.17	219	210
22R-Trishomohopane	8.65	4.17	4.17	149	148
αββ-20R-C27-Cholestane	8.65	4.17	4.17	201	146
αββ-20S-C27-Cholestane	8.65	4.17	4.17	234	212
ααα-20S-C27-Cholestane	8.65	4.17	4.17	260	241
αββ-20R-C28-Ergostane	8.65	4.17	4.17	172	159
αββ-20S-C28-Ergostane	8.65	4.17	4.17	186	176
αββ-20R-C29-Sitostane	8.65	4.17	4.17	428	375
αββ-20S-C29-Sitostane	8.65	4.17	4.17	421	394

a — rows Na through Pb
b — rows Phenanthrene through Coronene
c — rows 17α(H)-22,29,30-Trisnorhopane through αββ-20S-C29-Sitostane

	Accord Diesel	DPF-Accord	Corolla Gasoline	Golf Diesel	Golf Biodiesel
Tetradecane	338	94.6	93.4	173	168
Pentadecane	938	92.7	92.7	211	195
Hexadecane	2320	227	225	485	440
Norpristane	516	81.1	81.1	165	165
Heptadecane	1990	394	393	946	854
Pristane	307	102	101	214	211
Octadecane	3400	1060	1070	4400	2290
Phytane	781	335	333	935	681
Nonadecane	5640	2380	2360	13000	5220
Eicosane	7780	3780	3740	19800	8140
Heneicosane	4000	2000	2070	18600	3900
Docosane	2180	1090	1260	13900	3040
Tricosane	1080	532	633	6640	1460
Tetracosane	567	315	387	4980	1360
Pentacosane	215	93.3	117	2950	956
Hexacosane	173	90.2	76.4	1240	104
Heptacosane	194	103	79.2	484	164
Octacosane	128	74.6	58.3	121	121
Nonacosane	147	86.9	70.8	147	147
Triacontane	147	89.2	70.8	147	147
Hentriacontane	208	118	100	208	208
Dotriacontane	216	109	104	216	216
Tritriacontane	242	126	117	242	242
Tetratriacontane	208	100	100	208	208
Pentatriacontane	208	100	100	208	208
Hexatriacontane	208	100	100	208	208
Heptatriacontane	251	121	121	251	251
Octatriacontane	260	125	125	260	260
Nonatriacontane	303	146	146	303	303
Tetracontane	329	158	158	329	329
Decylcyclohexane	93.9	4.17	4.17	8.65	8.65
Pentadecylcyclohexane	188	97.8	98.2	830	286
Hexadecylcyclohexane	42	25.2	30.9	614	382
Heptadecylcyclohexane	17	14.5	22.9	740	393
Octanoic acid	977	477	487	931	1890
Decanoic acid	1020	527	548	1050	1000
Dodecanoic acid	819	475	468	1300	876
Tetradecanoic acid	1180	652	656	1590	1540
Pentadecanoic acid	568	304	354	951	765
Hexadecanoic acid	6200	3510	3400	14100	95400
Heptadecanoic acid	209	115	126	461	1250
Octadecanoic acid	2990	1730	1750	4710	74500
Nonadecanoic acid	160	78.7	85.5	283	327
Pinonic acid	147	70.8	70.8	147	147
Palmitoleic acid	887	427	427	887	887
Oleic acid	1420	695	688	9500	87200
Linoleic acid	1360	672	672	5960	175000
Linolenic acid	260	125	125	808	260
Eicosanoic acid	114	64.5	69.1	380	5680
Heneicosanoic acid	233	113	113	272	582
Docosanoic acid	199	101	103	382	5100
Tricosanoic acid	117	57.0	59.6	174	643
Tetracosanoic acid	276	136	140	326	1950
Pentacosanoic acid	149	79.3	80.3	171	289
Hexacosanoic acid	170	82.2	82.9	183	310
Heptacosanoic acid	173	83.3	83.3	173	187
Octacosanoic acid	350	169	173	368	371
ROS	815	801	1260	1130	1020
DTT	109	2.6	4.8	432	248

d

e

f